NASA Contractor Report CR-180805

Aero/Structural Tailoring of Engine Blades (Aero/STAEBL)

Interim Report

K. Brown
UNITED TECHNOLOGIES CORPORATION
Pratt & Whitney
East Hartford, Connecticut

March 1988

Prepared for
Lewis Research Center
Under Contract NAS3-22525

National Aeronautics and
Space Administration

NASA National Aeronautics and Space Administration

Report Documentation Page

1. Report No.	2. Government Accession No.	3. Recipient's Catalog No.
NASA CR-180805		

4. Title and Subtitle	5. Report Date
Aero/Structural Tailoring of Engine Blades (AERO/STAEBL) Interim Report	March 1988
	6. Performing Organization Code

7. Author(s)	8. Performing Organization Report No.
K. W. Brown	PWA-5774-82
	10. Work Unit No.

9. Performing Organization Name and Address	11. Contract or Grant No.
UNITED TECHNOLOGIES CORPORATION Pratt & Whitney, Commercial Engine Business 400 Main St., East Hartford, CT 06108	NAS3-22525
	13. Type of Report and Period Covered
12. Sponsoring Agency Name and Address	Contract Report
NATIONAL AERONAUTICS AND SPACE ADMINISTRATION Lewis Research Center 21000 Brookpark Road, Cleveland, Ohio 44135	14. Sponsoring Agency Code

15. Supplementary Notes

Project Manager: C. C. Chamis, Mail Stop 49-6
NASA-Lewis Research Center, Cleveland, Ohio

16. Abstract

This report describes the Aero/Structural Tailoring of Engine Blades (AERO/STAEBL) program, which is a computer code used to perform engine fan and compressor blade aero/structural numerical optimizations. These optimizations seek a blade design of minimum operating cost that satisfies realistic blade design constraints. This report documents the overall program (e.g., input, optimization procedures, approximate analyses, etc.) and also provides a detailed description of the validation test cases.

17. Key Words (Suggested by Author(s))	18. Distribution Statement
Approximate Analysis; Mathematical Optimization; Objective Function; Refined Analysis	

19. Security Classif. (of this report)	20. Security Classif. (of this page)	21. No. of pages	22. Price
Unclassified	Unclassified	62	

NASA FORM 1626 OCT 86

TABLE OF CONTENTS

TABLE OF CONTENTS (continued)

LIST OF ILLUSTRATIONS

LIST OF TABLES

SECTION 1.0

SUMMARY

The objective of the Aero/Structural Tailoring of Engine Blades (AERO/STAEBL) program is to develop a computer code capable of performing engine fan and compressor blade aero/structural numerical optimizations. These optimizations seek a blade design of minimum operating cost that satisfies realistic blade design constraints, by tuning from two to thirty aerodynamic and structural blade design variables.

The design constraints of AERO/STAEBL include blade stresses, blade forced vibratory response, flutter, and foreign object damage. Blade design variables include airfoil thickness at up to five locations, inlet air angle, number of blades, blade chord, edge radius, blade stacking, and internal construction including hole size for hollow blades, and, for composite blades, ply thickness and orientation angle.

To perform a blade optimization, three component analysis categories are required: an optimization algorithm; approximate analysis procedures for objective function and constraint evaluation; and refined analysis procedures for constraint recalibration and optimum design validation. The optimization algorithm of AERO/STAEBL is the ADS (Automated Design Synthesis) optimization package. ADS has the flexibility of providing many different optimization algorithms with no change of software requirements, and is a well accepted and proven tool for optimizations employing a small to medium (1 to 30) number of design variables.

The approximate analyses of AERO/STAEBL are focused upon an efficient, coarse mesh, plate finite element blade vibration analysis procedure. From an aerodynamic description of the blade, rotor efficiency and blade coordinates are generated. A mesh generator is then accessed to create a finite element mesh. The finite element analysis provides blade weight, stresses under centrifugal loads, blade natural frequencies, mode shapes, and modal speed sensitivities. Additional constraint evaluations, including flutter and foreign object damage stress calculations, utilize frequency and mode shape output from the finite element analysis.

When a candidate optimum design is obtained, the results of the approximate structural analyses are checked by performing a refined finite element analysis using the NASTRAN (NASA STRuctural ANalysis) code, and a converged finite element mesh. Execution of the analysis check is performed manually, although AERO/STAEBL provides the finite element model for the refined analysis.

Verifications of the AERO/STAEBL code were conducted using the fan stage and the sixth compressor stage of the Energy Efficient Engine, which were designed under NASA Contract NAS3-20646. In each verification, the final blade design served as a starting point for the subsequent AERO/STAEBL optimizations. In each case, significant potential for savings was demonstrated through the application of optimization and through the use of advanced composites.

Blade structural design tailoring, as performed by AERO/STAEBL, has been demonstrated to be a very powerful automated design procedure through applications to the Energy Efficient Engine fan and compressor. AERO/STAEBL provides the computational capability to simultaneously evaluate many design variables to optimize a comprehensive objective function while satisfying numerous design requirements.

SECTION 2.0

INTRODUCTION

Fan and compressor blades are designed to provide aerodynamic performance and structural durability through aerodynamic and structural design iterations. These design iterations require that specific design criteria, determined through empirical correlations, must be satisfied. The aerodynamics engineer seeks a blade that has maximum performance, regardless of the airfoil durability. The structural designer, on the other hand, must design a blade which is structurally durable with little or no penalty in performance. To design a structurally durable blade, the structural designer interactively conducts vibration, steady state stress, and ingestion analyses of proposed designs, allows design modification for reanalysis, compares results of analysis with design criteria, and assembles the input required to perform non-interactive flight cycle life analysis. Often, the blade designer must use personal experience and intuition to establish which path to follow to improve a design, and to decide when a design is adequate.

Once the structural engineer has found a blade that satisfies the structural durability requirements (constraints), it must be sent back to the aero group for efficiency evaluation. Often, the aerodynamicist will make slight changes to the blade to try and maintain flow area, efficiency and thrust. The blade must be again analyzed by the structural engineer, perturbed, and passed back to aero. Thus, a blade may go through several inter-group iterations, lasting over a period of several months. By including both the aerodynamic and structural evaluations within AERO/STAEBL, these inter-group iterations are greatly reduced or even eliminated.

Thus, current turbine engine blade design procedures are partly engineering and partly art. The quality of a design is often dependent on the judgement and experience of the engineering team that performed the design task. The penalties for these less than optimum designs are increased engine weight and cost, including decreased efficiency, and needlessly long development cycles, due to the need to fix failures and improve engine performance. Correcting a problem is always more expensive than designing it correctly initially, when constraints are less rigid. Once a design fault has been corrected, it is usually at the expense of engine cost or weight. Thus, degradation of the overall engine performance is generally the result.

It is apparent that current blade design procedures require a team of experienced design engineers to decide what are appropriate trade-offs during the blade design process. The purpose of the Aero/Structural Tailoring of Engine Blades (AERO/STAEBL) program is to formalize the structural blade design procedure. Such formalized optimum design procedures have been developed and used with considerable success for optimum structural design of linear static structures, and are now being used with some success for the aeroelastic tailoring of fixed aircraft wings. The AERO/STAEBL procedure can reduce human error and increase productivity in the blade design process by automating what was formerly a cumbersome, judgemental design process.

The capabilities of the automated design procedure have been demonstrated through its application to fan blades made from advanced composites, as well as to a standard, shroudless compressor stage. The design optimization of these complex structures was a rigorous test of the AERO/STAEBL program.

To meet the objective of the AERO/STAEBL program, seventeen technical tasks were established as part of NASA Contract NAS3-22525:

Task I - AERO/STAEBL Procedure: Design of the general AERO/STAEBL procedure

Task II - Input: Definition of AERO/STAEBL procedure input parameters including initial blade geometry, material properties, loads, weight and cost models, and design constraints

Task III - Approximate Analyses: Modification of existing beam analyses to perform vibration, stress and foreign object damage evaluations of composite blades

Task IV - Optimization Procedure: Identify a procedure which optimizes the objective function, direct operating cost plus interest, within limits of specified constraints

Task V - Refined Analyses: Establish a procedure for using NASTRAN to validate optimized blade designs

Task VI - Demonstration and Documentation: Demonstrate and document the AERO/STAEBL procedure by using it to tailor two alternate designs of the shroudless Energy Efficient Engine fan blade: (1) a solid blade made from superhybrid composites, and (2) a hollow blade with metal-matrix composite inlays

Task VII - Approximate Analysis: Modify the existing AERO/STAEBL code to include plate finite elements for approximate stress, vibration, and local ingestion analysis

Task VIII - AERO/STAEBL Computer Program Development: Assembly of the improved analyses for the Aero/Structural Tailoring of Engine Blades, including provisions for input, optimization using approximate analysis, output, and communication links for refined analysis

Task IX - AERO/STAEBL Computer Program Validation: Optimize four test cases to demonstrate and validate the AERO/STAEBL Computer Program, including a typical compressor blade

Task X - AERO/STAEBL Computer Program Documentation: Assemble a Theoretical Manual and a User's Manual for the AERO/STAEBL program to describe the approximate analysis techniques used in the program and to present user instructions and guidelines

Task XI - AERO/STAEBL Computer Program Delivery: Deliver the AERO/STAEBL computer program to NASA, install on NASA's IBM 370 computer, and validate successful program operation

Task XII - Selection of Design Variables, Constraints and Objective Function: Incorporate additional design variables and appropriate blade performance constraints to AERO/STAEBL to provide the freedom to develop an optimum aero/structural design; modify the objective function to include blade performance in the operating cost evaluation

Task XIII - Aerodynamic Analyses: Add approximate and refined aerodynamic analyses to the AERO/STAEBL optimization system; include a blade geometry generator, and an aerodynamic loss calculation

Task XIV - AERO/STAEBL System Modification: Incorporate an improved optimizer in the AERO/STAEBL system, along with the approximate aerodynamic analysis; reconfigure AERO/STAEBL for use of the ADS (Automated Design Synthesis) optimizer

Task XV - AERO/STAEBL Procedure Modification: Modify the AERO/STAEBL analysis to include the aerodynamic analysis of engine blades; identify specific aero/structural optimization strategies

Task XVI - Aero/Structural Tailoring Validation: Validate the enhanced AERO/STAEBL system

Task XVII - Aero/Structural Tailoring System Documentation, Delivery, and Demonstration: Update the AERO/STAEBL Theoretical and User's Manuals; install and validate the new system on the NASA-Lewis Research Center CRAY computer; conduct a seminar to discuss the theory and application of the AERO/STAEBL system.

The facility used for the AERO/STAEBL program was an IBM 370 computing system. Using IBM's latest virtual storage technology, five different IBM computers accommodate fully computerized interactive design systems, general time-sharing, teleprocessing, real time management/information systems, and management and scientific batch processing.

SECTION 3.0

OVERVIEW

Airfoil structural design is a critical part of the aircraft turbine engine development process. The limitations imposed by durability requirements for the airfoils have a direct bearing on the aerodynamic performance that can be achieved. In addition, a significant portion of engine weight and engine cost is a simple multiple of airfoil weight. The airfoil design problem is indeed a complex one. Chord, thicknesses at several locations, blade tilt, and internal constructions are selected to simultaneously satisfy vibration, ingestion, and flight cycle durability requirements. Mathematical programming techniques have been developed to expedite solution of this kind of tailoring problem which involves many design variables and many requirements. The airfoil application is particularly appropriate because the complex shapes defined by optimization do not increase manufacturing cost. The basic aerodynamic shapes are fabricated in accordance with three-dimensional numerical definitions which are readily modified to accept the results of structural tailoring.

Problems associated with structural tailoring of engine blades include: (1) engine blades are designed to operate in a dynamic environment by application of constraints which differ substantially from those applied to linear static structures; (2) analysts and/or designers have hesitated to develop optimization procedures for blades made from homogeneous materials because acceptable designs can be derived from past experience; and (3) finite element analyses, which are too time consuming to be used effectively in an optimization procedure, have been used in designing blades having advanced constructions such as those to be designed in this program.

Figure 1 summarizes the procedure employed for the Aero/Structural Tailoring of Engine Blades. Design variables are initiated by input to the procedure and are varied during the optimization. Approximate analyses for low cycle fatigue, flutter, resonance, and foreign object damage are applied to evaluate their effects relative to constraints.

The objective function that is minimized in the AERO/STAEBL procedure is derived from the relationships illustrated in Figure 2. The complexity encountered in finding the design which minimizes this function can be illustrated by examining its relationship to blade chord (Figure 3). It appears to be a simple process, but the minimization becomes complicated when structural constraints are introduced (Figure 4). The design that the procedure selects must minimize user costs without violating these imposed constraints.

The ADS (Automated Design Synthesis) optimization program was selected as the most effective available technique for solving nonlinear optimization problems. The ADS program is a general purpose optimization algorithm that includes a wide variety of optimizers (Reference 1).

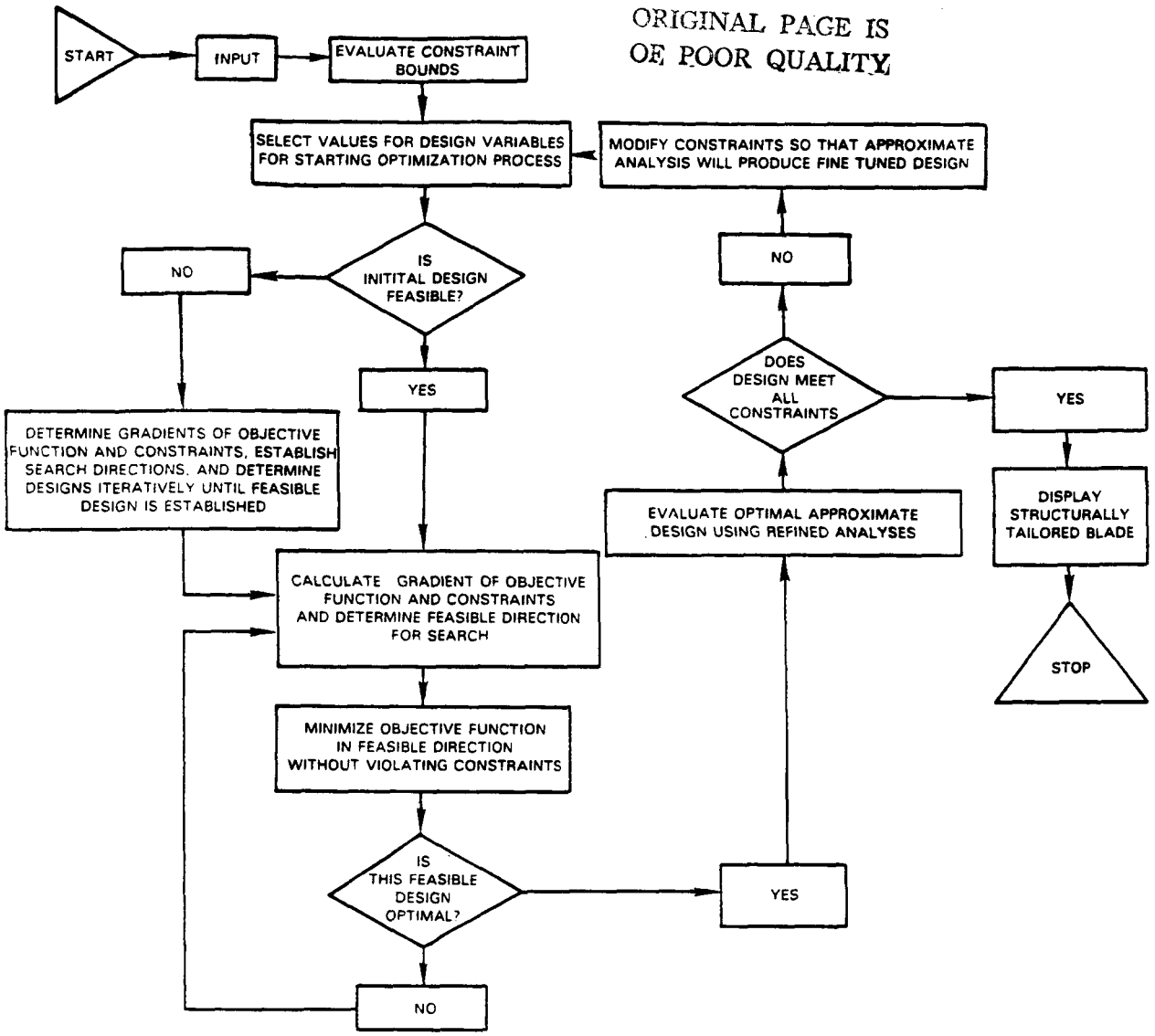

Figure 1 The Aero/Structural Tailoring of Engine Blades Procedure

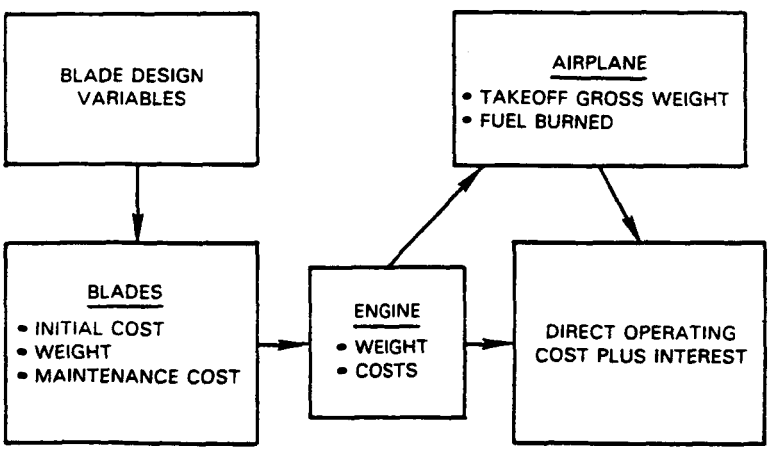

Figure 2 The Objective Function Relates Airline Economics to Blade Design Variables

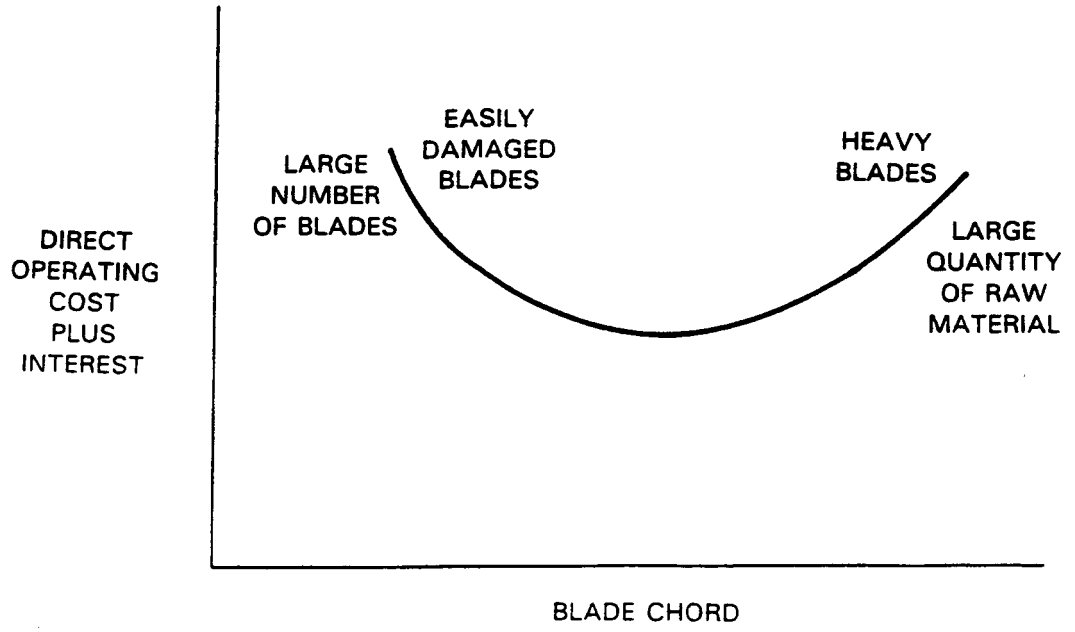

Figure 3 Blade Chord Optimization Appears to be a Simple Design Problem

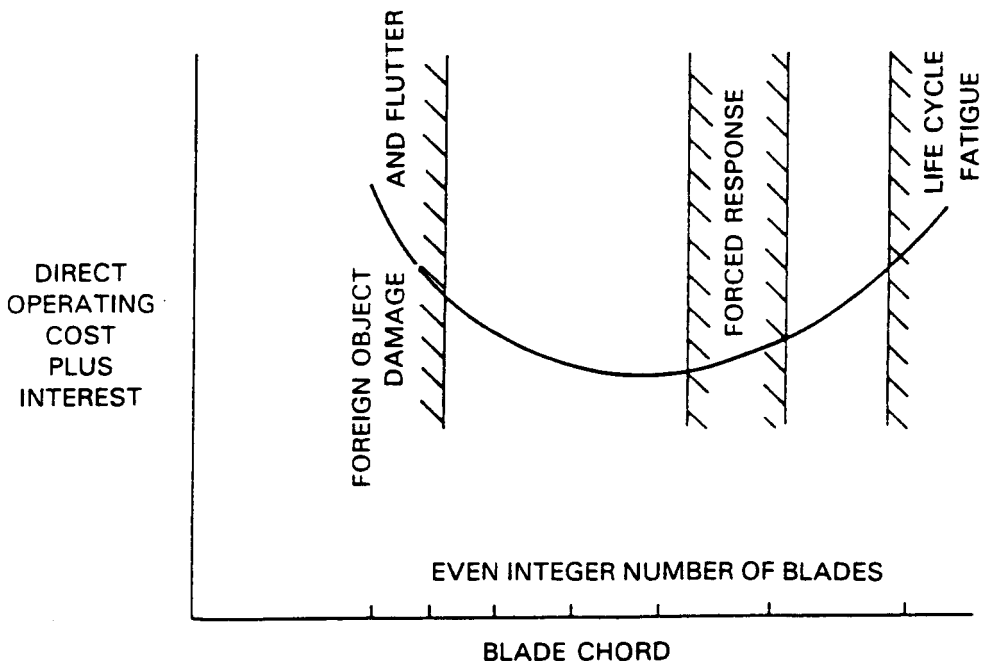

Figure 4 Design Problem Complexity Is Introduced by Structural Constraints (Disjointed Design Space)

The aero/structural methodologies embedded in the AERO/STAEBL procedure identify a fine-tuned optimum blade design that is validated by NASTRAN refined analysis. The procedure was demonstrated by the design of two composite material shroudless fan blades, and also for a metallic compressor blade.

The AERO/STAEBL computer code generally reduces human error in the blade design process by automating with mathematical precision what was formerly user judgement in a long, tedious, interdiscipline interactive process.

SECTION 4.0

INPUT

To perform an optimization using the AERO/STAEBL system, an initial geometry must be defined. Due to the complexity of AERO/STAEBL, this initial set of definitions must include the rotor geometry (including blade and attachment geometries), the aerodynamic operating conditions, and the materials under consideration. To perform an optimization, further definitions are required, including the function to minimize (objective function), constraints which must be satisfied, and parameters (design variables) which are available to the optimization process. Table I summarizes the features available within the AERO/STAEBL system, including available design variables, behavior variables, constraints, side constraints, and gradient information.

Table I

AERO/STAEBL Optimization Features

Design Variables	Behavior Variables	Constraints
Chord	Weight	Frequency
Thickness/Chord	Efficiency	Stress
Composite Material (Hollow) Loc	Angle of Twist	Aero Log Dec
Inlet Air Angle	Camber	Untwist Defl
Number of Blades	Frequency	
Axial Tilt	Stress	
Tangential Tilt	Flutter Damping Coef	

Side Constraints	Gradients (for Sensitivity Analysis)
Max, Min Limits for Design Variables	$\frac{d(obj)}{d(var)}$, $\frac{d(constraint)}{d(var)}$

4.1 AERODYNAMIC STAGE

The starting point for structural tailoring of an engine blade is a candidate aerodynamic stage design which will deliver the required airflow and pressure ratio. The aerodynamic description of this candidate design is input to the structural tailoring procedure in the following form:

- Aerodynamic definitions of a series of airfoil sections (used to define airflow conditions, stagger, camber, edge radii, chord and thickness, all of which are functions of radius)
- Flowpath boundaries (root and tip radii and convergence angles)
- Number of blades.

4.2 SUPPORT STRUCTURE

The dominant variables which control structural tailoring are frequency dependent and sensitive to blade attachment flexibility. Since the space available for the attachment varies with the airfoil design parameters, attachment flexibility is recognized by increasing the effective length of the candidate aerodynamic blade design. The additional input is:

- Effective inner radius
- Dimensions of a rectangular section in the extended region.

4.3 OPERATING CONDITIONS

Airfoil peak steady stress is calculated at maximum normal speed to determine life. Fatigue is prevented by tuning to avoid critical resonances at any speed above minimum cruise. Flutter stability and response to ingestion of a standard size bird are calculated at maximum takeoff rotor speed. The input required to make these calculations is:

- Rotor speeds
- Relative flow velocity, Mach number, incidence and density.

4.4 MATERIALS

Blade centrifugal stresses and vibratory characteristics result from body loads and are, therefore, fully dependent upon the properties of the blade materials. Blade life is dependent on the strength of the material subjected to a particular stress condition. Composite materials, such as those to be used in the blades tailored in this program, are composed of a fixed portion of fiber and matrix constituents and can be considered to be homogeneous materials with directional properties. Similarly, adhesively bonded plies of metal matrix composite can be considered to be a single material. The net criticality of a local stress state is determined by evaluating a parameter which is a function of the relative criticality of each individual stress component. The input which defines the required properties for each material is:

- Density
- Directional moduli and Poisson's ratios
- Directional cyclic strengths.

4.5 OBJECTIVE FUNCTION

The AERO/STAEBL procedure optimizes a single benefit which can be related to the final design. The benefit may be as simple as airfoil weight or it may be total value to the engine operator which considers trades between weight, initial cost, maintenance cost and even areodynamic performance. The benefit expression is kept in generalized form by introducing a FORTRAN definition of:

- An objective function of design variables or quantities which are defined by the design variables (constant terms are not required).

4.6 CONSTRAINTS

The durability objectives of a blade design are accomplished by imposing limits on the quantities that are calculated in the structural analyses. Margins are established relative to idealized limits to recognize the effects of geometric, material, and operational tolerances and to compensate for approximations in the analyses or underlying assumptions. The input to the AERO/STAEBL procedure is:

- Minimum allowable predicted aerodynamic damping
- Minimum allowable difference between predicted frequencies and critical multiples of rotor speed
- Maximum allowable local and root bird ingestion stress parameters
- Limits on design variables (to guarantee airfoil fabricability and erosion resistance).

4.7 DESIGN VARIABLES

Scaling techniques are provided within the AERO/STAEBL procedure to vary the coordinates that define any airfoil section in proportion with changes in chord or maximum thickness (fairing to proper edge radii). Logic has also been included to identify the particular material at any point in a composite blade by references to quantities which define the relative position of the limits of that material. A fiber orientation angle is associated with each composite material. The relevant input is: (1) coded identification of design variables, and (2) initial values for starting the iteration, and includes:

- Airfoil chord (splined between defined variable stations)
- Thickness/chord
- Composite material location limits (including the cavity as a zero properties composite)

- o Composite material fiber orientation angles
- o Inlet relative airflow angle
- o Number of blades
- o Axial and tangential tilts.

By varying the inlet relative airflow angle, AERO/STAEBL is able to vary the airfoil angle of twist, and also the camber. Since the AERO/STAEBL analysis assumes that the upstream and downstream aerodynamics will be unchanged by the optimization, a change in inlet relative airflow angle results in a change of angle of twist. To maintain the proper downstream aerodynamic conditions, the airflow trailing angle must remain constant, hence requiring a change of camber. Thus, angle of twist and camber are treated as dependent, or behavior, variables in AERO/STAEBL. Airfoils are stacked on the cross section centers of gravity in the AERO/STAEBL airfoil finite element mesh generator. From this reference, sections may be offset both axially and tangentially, through tilt variables. Usage of this tilting capability can be helpful in reducing bending stresses caused by gas pressure on the airfoil.

SECTION 5.0

OPTIMIZATION PROCEDURES

A common engineering design problem is the determination of values for design variables which minimize a design quantity such as weight, drag, or cost, while satisfying a set of auxiliary conditions. In the AERO/STAEBL program, the structural design of a composite or hollow fan blade is accomplished by varying airfoil section thicknesses, chord, titanium skin thickness, etc., to minimize a combination of weight and cost subject to constraints on resonance, flutter, stress, and foreign object damage.

5.1 GENERAL OPTIMIZATION THEORY AND BACKGROUND

The engineering design process can be modeled as a mathematical programming problem in optimization theory. In theoretical terms, this constrained minimization problem can be expressed as follows:

$$\text{minimize } f(\underline{x}), \tag{1}$$

subject to the auxiliary conditions,

$$g_i(\underline{x}) \leq 0, \; i=1, \ldots, m. \tag{2}$$

The quantity $\underline{x} = (x_1, \ldots, x_n)$ is the vector of n design variables. The scalar function to be minimized, $f(\underline{x})$, is the objective function; and $g_i(\underline{x}) \leq 0$, i=1, ..., m are the m inequality constraints. Upper and lower bounds on the design variables, e.g.,

$$L_i \leq x_i \leq U_i, \; i=1, \ldots, n, \tag{3}$$

are referred to as side constraints. The n-dimensional space spanned by the design variables defines the design space. If $f(\underline{x})$ and $g_i(x)$, i=1, ..., m, are all linear functions of $\underline{x}$, the optimization problem is a linear problem (LP) which can be solved by well known techniques, such as Dantzig's simplex method. If $f(\underline{x})$ or any of the $g_i(\underline{x})$'s are nonlinear, then it is a nonlinear programming (NP) problem for which a number of solution techniques are also available. If the objective function, $f(\underline{x})$, is to be maximized, then the equivalent problem of minimizing $-f(\underline{x})$ is performed.

Any choice of variables, $\underline{x}$, in design space that satisfies all the constraints, (2) and (3), is a feasible point. As shown in Figure 5, the union of all feasible points comprises the feasible region. The locus of points which satisfy $g_i(\underline{x}) = 0$ for a particular i, forms a constraint surface. On one side of the surface, $g_i(\underline{x}) \leq 0$ and the constraint is satisfied; on the other side, $g_i(\underline{x}) \geq 0$ and the constraint is violated. Points on the interior of the feasible region are free points; points on the boundary are bound (constrained) points. If it is composed of two or more distinct sets, the feasible region is disjoint. A design point in the feasible region that

minimizes the objective function is an optimal feasible point and is a solution of the problem posed in (1) through (3). As in any nonlinear minimization problem, there can be multiple local minima. In this case, the global minimum is the optimal feasible point. If a design point is on a constraint surface (i.e., $g_i(\underline{x}) = 0$ for some i), then that particular constraint is active. A solution to a structural optimization problem is almost always on the boundary of the feasible region, and is usually at the intersection of two or more constraint surfaces (i.e., there are two or more active constraints).

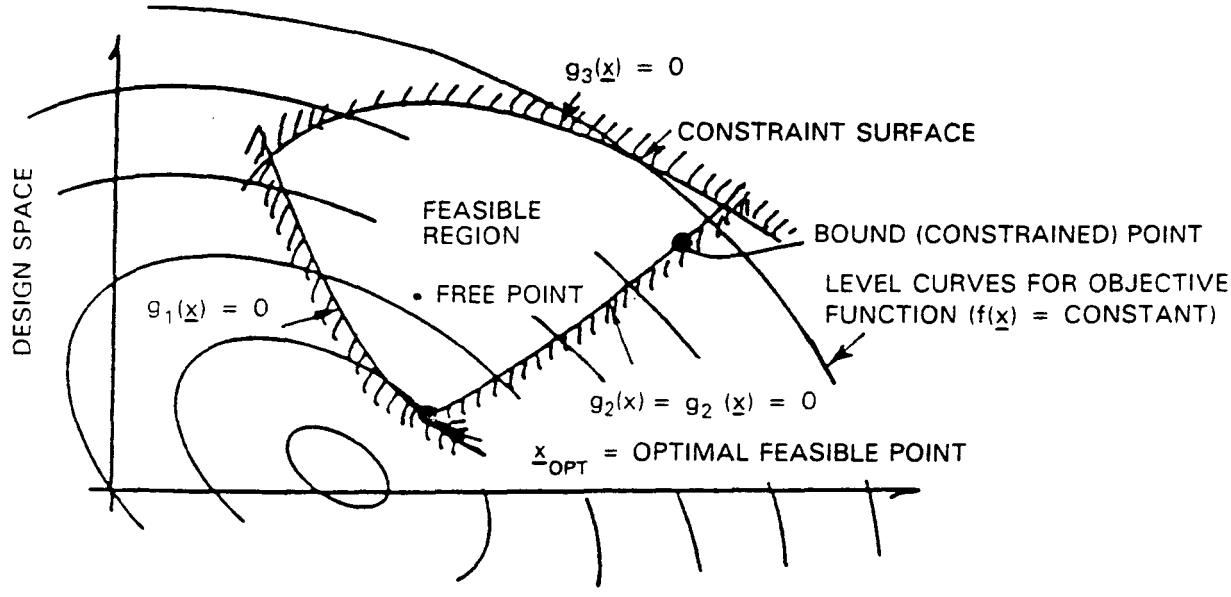

Figure 5 Feasible Region Is Union of All Points that Satisfy All Constraints

There are two basic approaches to solving the constrained optimization problem posed in (1) through (3): direct methods (e.g., methods of feasible directions) and indirect methods (e.g., penalty function methods).

In a direct method, the objective function and constraints are evaluated independently, and the constraints are treated as limiting surfaces. Zoutendijk's method of feasible directions is an example of a direct method.

In an indirect method, the problem is reformulated so that (1) through (3) are replaced by a single unconstrained optimization problem. For example, in an exterior penalty function method, violations of the constraints are added onto the objective function to form an augmented objective function. If a constraint is violated, a penalty term is added onto the objective function. By minimizing the objective function subject to increasing values of the penalty parameter, the optimum may be obtained. One advantage of this approach is that each of the successive minimization problems can be solved using a

standard unconstrained function minimization technique, such as a conjugate gradient or quasi-Newton method. Computationally, however, the process is not usually competitive with direct procedures.

Many optimization software packages are available in software libraries (e.g., the International Mathematical and Statistic Libraries, Inc., and HARWELL) that can solve the constrained minimization problem using either direct or indirect techniques. The ADS (Automated Design Synthesis) computer program (Reference 1) was selected for the AERO/STAEBL blade optimization application due to its proven success and versatility in solving structural optimization problems.

5.2 AERO/STAEBL ADS IMPLEMENTATION

ADS is a general purpose numerical optimization program containing a wide variety of optimization algorithms. The solution of the optimization problem has been divided into three basic levels by ADS: (1) strategy, (2) optimizer, and (3) one-dimensional search. By allowing the user to select the strategy, optimizer, and one-dimensional search procedure, considerable flexibility is provided for finding an optimization algorithm which works well for the specific design problem being solved.

Strategy

The optimization strategies available in AERO/STAEBL are listed in Table II. The parameter ISTRAT is sent to the ADS program to identify the strategy selected by the user. Selecting the ISTRAT=0 option transfers control directly to the optimizer. This is selected when choosing the Method of Feasible Directions or the Modified Method of Feasible Directions for solving the constrained optimization problem.

Table II

ADS Strategy Options

ISTRAT	Strategy to be Used
0	None. Go directly to the optimizer
1	Sequential unconstrained minimization using the exterior penalty function method
2	Sequential unconstrained minimization using the linear extended interior penalty function method
3	Sequential unconstrained minimization using the quadratic extended interior penalty function method
4	Sequential unconstrained minimization using the cubic extended interior penalty function method
5	Augmented Lagrange Multiplier Method
6	Sequential linear programming
7	Method of Centers
8	Sequential quadratic programming
9	Sequential convex programming

Optimizer

The IOPT parameter selects the optimizer to be used by ADS. Table III lists the optimizers available within AERO/STAEBL. Note that not all optimizers are available for all strategies. Allowable combinations are shown on Table V.

Table III

ADS Optimizer Options

IOPT	Optimizer to be Used
1	Fletcher-Reeves algorithm for unconstrained minimization
2	Davidon-Fletcher-Powell (DFP) variable metric method for unconstrained minimization
3	Broydon-Fletcher-Goldfarb-Shanno (BFGS) variable metric method for unconstrained minimization
4	Method of Feasible Directions for constrained minimization
5	Modified Method of Feasible Directions for constrained minimization

One-Dimensional Search

Table IV lists the one-dimensional search options available for unconstrained and constrained optimization problems. The parameter ISERCH selects the search algorithm to be used.

Table IV

ADS One-Dimensional Search Options

ISERCH	One-Dimensional Search Option
1	Find the minimum of an unconstrained function using the Golden Section method
2	Find the minimum of an unconstrained function using the Golden Section method followed by polynomial interpolation
3	Find the minimum of an unconstrained function by first finding bounds and then using polynomial interpolation
4	Find the minimum of an unconstrained function by polynomial interpolation/extrapolation without first finding bounds on the solution
5	Find the minimum of a constrained function using the Golden Section method
6	Find the minimum of a constrained function using the Golden Section method followed by polynomial interpolation
7	Find the minimum of a constrained function by first finding bounds and then using polynomial interpolation
8	Find the minimum of a constrained function by polynomial interpolation/extrapolation without first finding bounds on the solution

Allowable Combinations of Algorithms

Not all combinations of strategy, optimizer, and one-dimensional search are meaningful. For example, it is not meaningful to use a constrained one-dimensional search when minimizing unconstrained functions. Table V identifies those combinations of algorithms which are meaningful in the AERO/STAEBL program. In this table, an X is used to denote an acceptable combination of strategy, optimizer, and one-dimensional search, while an O indicates an unacceptable choice of algorithm. To use the table, start by selecting a strategy. Read across to determine the admissable optimizers for that strategy. Then, read down to determine the acceptable one-dimensional search procedures. From the table, it is clear that a large number of possible combinations of algorithms is available.

Table V

ADS Program Options

	Optimizer				
Strategy	1	2	3	4	5
0	X	X	X	X	X
1	X	X	X	0	0
2	X	X	X	0	0
3	X	X	X	0	0
4	X	X	X	0	0
5	X	X	X	0	0
6	0	0	0	X	X
7	0	0	0	X	X
8	0	0	0	X	X
9	0	0	0	X	X
One-Dimensional Search					
1	X	X	X	0	0
2	X	X	X	0	0
3	X	X	X	0	0
4	X	X	X	0	0
5	0	0	0	X	X
6	0	0	0	X	X
7	0	0	0	X	X
8	0	0	0	X	X

X = Acceptable
0 = Not Acceptable

5.3 OPTIMIZER COMPARISON

A simplistic comparison of the optimization algorithms available to the ADS program was conducted by optimizing a simple beam. The problem is to minimize the weight of a rectangular cross-section cantilever beam under bending load, subject to bending stress, shear stress, aspect ratio, and deflection constraints. A sample of the options available in the ADS program was run, as detailed in Table VI. As can be seen from the table, the feasible directions and the modified feasible directions procedures are among the most efficient optimization algorithms yet developed. This trend has also applied to the AERO/STAEBL optimizations conducted to date.

Table VI

ADS Optimization Algorithm Comparison

ISTRAT	IOPT	ISERCH	Funct. Calls	Min. Wt.
0	4	7	21	6763
0	4	5	46	6525
0	5	5	43	6637
0	5	6	43	6637
0	5	7	29	6603
0	5	8	23	6574
1	1	8	62	8451
2	1	8	134	7440
3	1	8	137	7426
4	1	8	26	20000
5	1	8	55	10102
5	2	8	52	7445
5	3	8	56	7336
6	4	8	24	6613
6	5	8	24	6626
7	5	8	33	7548
8	5	8	34	6476
9	5	8	33	6757

5.4 ESTIMATED FUNCTION CALL REQUIREMENTS

A reasonable estimate for the number of analysis function calls, and hence the amount of computer time that will be required, may be made based on experience with the ADS optimizer and AERO/STAEBL. As indicated in Figure 5, each optimizer design iteration consists of a gradient evaluation of the objective function and constraints to determine the search direction, followed by a one-dimensional line search in that direction. When the gradients are not known analytically (as is the case for the AERO/STAEBL application), a backward difference gradient approximation is used. For n design variables, n function calls are required for the finite difference gradient calculation.

Method of Feasible Directions

The one-dimensional line search usually requires three additional function evaluations to update the objective function and constraints and to determine where the search should terminate. Thus, for m iterations, with n+3 function calls per iteration, we have:

$$N = m\ (n + 3)\ , \tag{4}$$

where N is the number of function evaluations required to determine the optimum design. Typically, convergence is attained in approximately 10 iterations, so that a good estimate for function call requirements is $N = 10\ n + 30$. Notably, N increases linearly with an increase in the number of design variables.

Modified Method of Feasible Directions

The modified method of feasible directions tends to follow the actual constraint surface more closely than does the method of feasible directions, and hence requires fewer design iterations, often converging in 4 or 5 iterations. This is done at the sacrifice of more moves along the one-dimensional line search, often taking 8 or 10 of these. In all, a reasonable estimate for function call requirements for this method is $N = 6\ n + 50$. Thus, for relatively large problems, this procedure promises to be more economical than the method of feasible directions. In practice, it is often useful to test each method, for at times one will achieve a superior design than the other, regardless of function call requirements.

5.5 ADS INTERFACE WITH AERO/STAEBL APPROXIMATE ANALYSES

The various AERO/STAEBL approximate analyses and the ADS optimizer are all called from the AERO/STAEBL executive routine. The output from ADS to the analyses is in the form of a design vector. This vector contains changes to the design variables. These changes are splined and added to the design curves, which are then used in the flutter, finite element, and other analyses. These analyses provide values that are used to calculate an objective function value and constraint values, which are used by ADS to determine the next design vector. This process continues until an optimum is reached. The overall program flow is detailed in Figure 6.

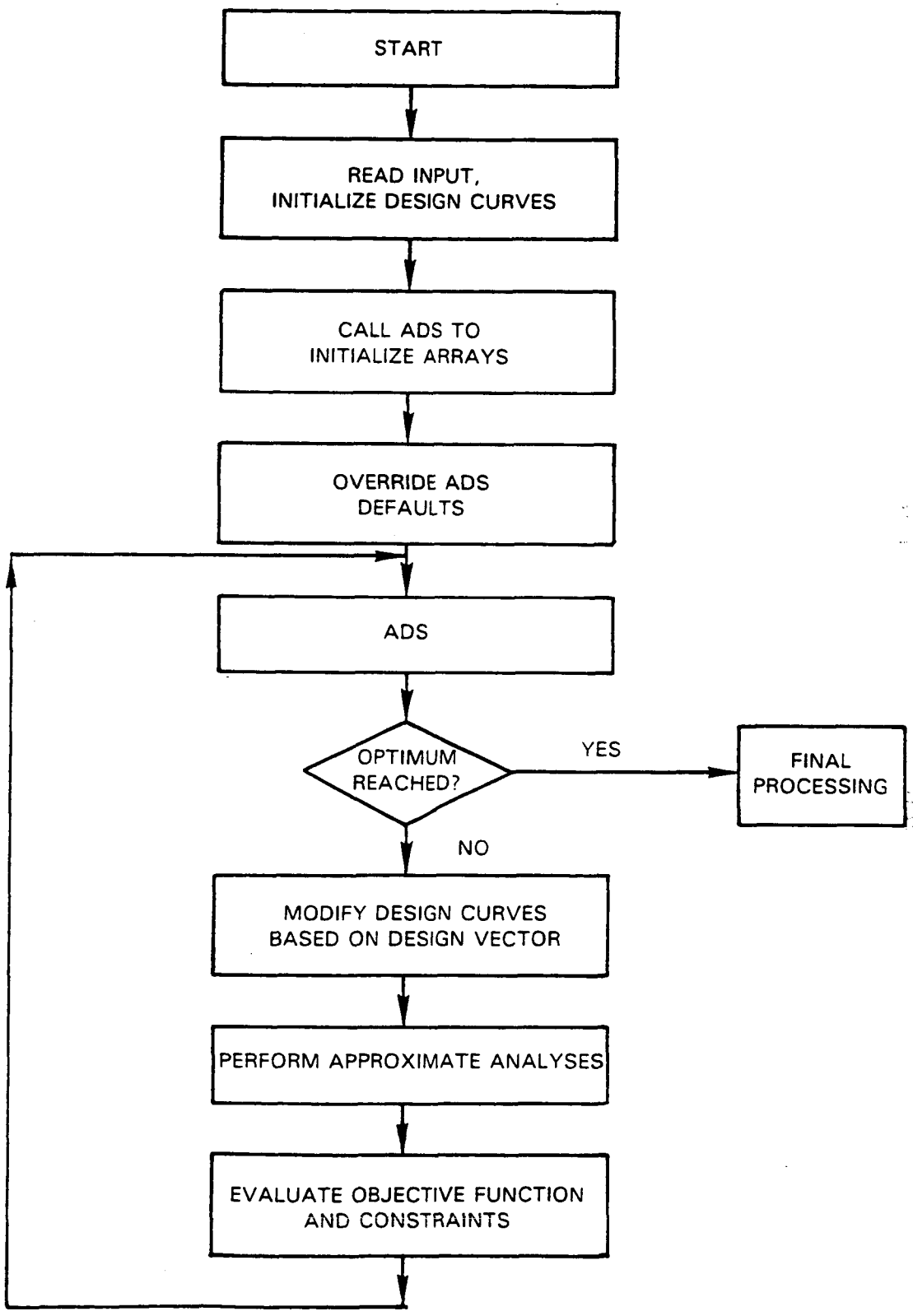

Figure 6 AERO/STAEBL Program Flow

SECTION 6.0

APPROXIMATE ANALYSES

Due to the many design iterations required to achieve an optimum blade configuration, many blade analyses must be performed. To derive candidate optima as efficiently as possible, blade optimizations are performed using approximate analysis procedures. These approximate procedures are efficient, fast running, and reasonably accurate. Once a candidate optimum has been achieved, the results of the approximate analyses are checked using more complex, refined analysis. Should the approximate and refined analyses agree, the design is a valid optimum. Should they disagree, the approximate analysis must be recalibrated, and the optimization process must be reinitiated. It is possible that the refined and the approximate analyses would not show increased agreement even after recalibration. This would mean that the approximate analysis was neglecting an important design parameter, and, as such, should be improved or replaced.

A detailed discussion of the approximate analyses is provided in the AERO/STAEBL Theoretical Manual (Reference 2). In the sections that follow, a brief review of these approximate analyses is presented.

To enable the application of plate finite element methodology to AERO/STAEBL approximate analysis, an efficient plate finite element procedure was created. The procedure uses NASTRAN methodology, but because of its reduced scale, all matrices may be stored in the computer's core, and all procedures take place in core. Thus, for the small meshes of the AERO/STAEBL approximate analysis, the special finite element code is able to deliver NASTRAN accuracy, but at greatly reduced computer expense. In fact, for most analyses, the plate methodology has proven to be more efficient than composite beam approximate analysis procedures.

6.1 AERODYNAMIC ANALYSIS

The AERO/STAEBL system has been constructed to allow for the aero/structural tailoring of an isolated rotor stage. Thus, all geometries of the rotor may be changed, and performance of the stage is a strong factor within the design objective function. Since the stage is isolated, upstream and downstream aerodynamics are fixed. Additionally, streamline locations are not allowed to move. While the absolute air angles are held fixed, the relative angles are free to change, however.

Because the leading edge flow need not be purely tangential, alterations on both blade camber and stacking (offset and twisting) are allowed. Sectional relative exit angles and camber angles are set for each geometry iteration by finding the camber angle that gives the proper absolute air exit angles. Air losses and exit total pressures are allowed to vary with each geometry iteration. Large deviations from the baseline airfoil are likely to entail performance losses, however.

Loss sources for the AERO/STAEBL aerodynamic analysis include: bow wave loss, tip supersonic loss, two-dimensional (2-D) low Mach number loss, incidence loss, throat area loss, and constant loss terms, including shock loss.

Net rotor efficiency is determined from flow averaged pressures and temperatures. The inlet pressures and temperatures and the exit temperatures are flow averaged from the baseline inlet and exit air streams.

6.2 BLADE MESH GENERATION

Due to the high number of approximate finite element analyses performed by the AERO/STAEBL system, efficient mesh generation is important. Additionally, mesh generation accuracy aids refined analysis calibration, and provides proper gradient information for the optimization scheme.

Using the circular arc airfoil definition, the aerodynamic analysis generates coordinates for each airfoil cross-section in a local chord-normal coordinate system. The AERO/STAEBL mesh generator stacks these sections on centers of gravity, with offsets for stacking variables. Blade stagger angles, also products of the aerodynamic analysis, define the angular section orientations.

Airfoil mesh generation requires the generation of section coordinates at arbitrary airfoil radial locations. In AERO/STAEBL this is accomplished by interpolating the scaled blade coordinates to generate coordinates at the required spanwise locations. From the interpolated coordinates, mean line coordinates are generated. For a selected number of chordwise elements, grid point locations and element thicknesses may then be generated. The finite element mesh is then loaded directly into the AERO/STAEBL work storage for utilization by the finite element program.

In creating models of conventional airfoils, special treatment is required at the blade root, where a neck of parallelogram cross-section serves to transition between the cambered airfoil and the dovetail that attaches the blade to the disk. Also, conventional blades have a platform at the airfoil to neck transition point to serve as the inner airflow seal. In AERO/STAEBL the extended neck is modeled using a row of plate finite elements. The platform is modeled using equivalent beam finite elements. The airfoil, platform and extended neck are joined together with rigid finite element constraint equations.

When modeling composite materials using plate finite elements, the standard procedure is to calculate equivalent membrane and bending material properties using lamination theory. AERO/STAEBL automates this approach, which enables the blade model to maintain the blade aerodynamic profile. To assure meaningful design variable gradients for optimization, AERO/STAEBL maps the layup of each element into a continuous, adjusted thickness, laminate.

6.3 FINITE ELEMENT STRESS AND VIBRATION ANALYSIS

Incorporation of finite element procedures for AERO/STAEBL approximate analysis required employing the most efficient solution procedures available. NASTRAN finite element methodology (Reference 3) was selected for use as the approximate analysis for several reasons:

- o Proven computational efficiency
- o Established successful correlations with test experience
- o Convenient input/output
- o Compatibility with NASTRAN refined analysis procedures.

The AERO/STAEBL finite element code has been generated specifically for blade vibratory and stress analysis. The program contains plate, beam and spring elements. For a given load condition, the AERO/STAEBL finite element program performs a static solution, a prestressed static solution, and a prestressed vibratory solution. Stresses, eigenvalues and eigenvectors are calculated.

The AERO/STAEBL finite element code is limited in scope; therefore, all solutions are performed in computer core, and are efficiently performed. Thus, solutions with plate analyses have become competitive with beam analyses in cost, but with improved accuracy.

The AERO/STAEBL plate element is a reduced integration triangular plate finite element, which includes the following features:

- o Recognition of thickness taper
- o Properly stacked triangular plate element meshes to simulate airfoil pretwist and camber
- o Composite material capabilities
- o Element differential stiffness
- o Lumped masses for storage efficiency.

6.3.1 Guyan Reduction

The Guyan reduction procedure has proven to be a very effective means for reducing the number of degrees-of-freedom used in the AERO/STAEBL dynamic analysis, while showing minimal loss of accuracy in the important lower modes. The procedure is based on the fact that many fewer grid points are needed to describe the inertia of a structure than are required to describe its stiffness with comparable accuracy. The reduction procedure, then, allows a condensation to occur, resulting in a much smaller equation set for dynamic analysis.

The use of relatively coarse finite element meshes in AERO/STAEBL coupled with the Guyan reduction procedure has been validated with both prismatic specimens and airfoils. Table VII shows flat plate frequency comparisons between a refined NASTRAN model and the coarse AERO/STAEBL analysis. The AERO/STAEBL model (run in NASTRAN for this comparison), reduced from 420 degrees-of-freedom to 36, gave very good frequency correlations relative to refined analysis, but consumed only 9.6 seconds of IBM 3081 central processing unit (CPU) time.

Table VII

Prismatic Cantilever Convergence Study with Guyan Reduction

Initial Degrees-of-Freedom	Degrees-of-Freedom After Reduction	NASTRAN CPU Time (seconds)	Deviation from Refined NASTRAN Solution (%) First Bending	First Torsion	Second Bending
900	84	24.5	0.0	0.0	0.0
900	45	18.9	0.0	0.2	0.2
420	36	9.6	-0.2	-1.2	-0.8

The efficiencies built into the AERO/STAEBL finite element model enable significant computer savings over NASTRAN. The third example of Table VII, which consumed 9.6 seconds in NASTRAN, gave identical frequency results in AERO/STAEBL, consuming only 3.6 seconds of computer time. The final Guyan reduced breakup, shown on Figure 7, reduces a 330 degree-of-freedom model to 24 degrees-of-freedom, which gives frequency results within 1.5 percent of the refined model in 2.3 seconds of computer time. This level of computer expense is well suited to optimization applications.

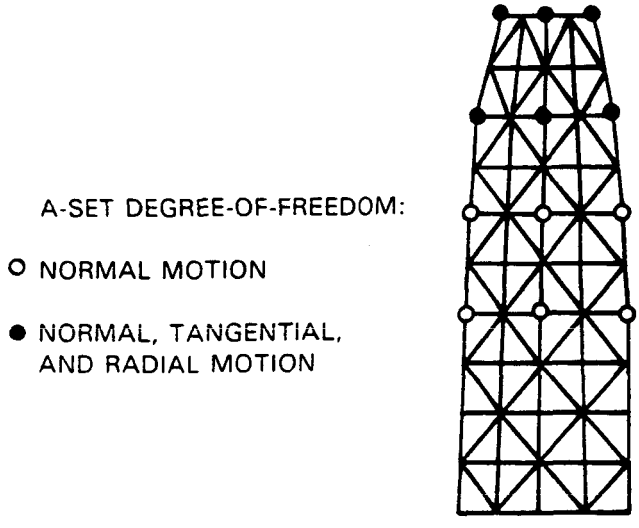

Figure 7 AERO/STAEBL Approximate Analysis Guyan Reduction Pattern

6.3.2 Static Stress Analysis

Within AERO/STAEBL, element stresses are recovered from the nodal deflections under static load for the statically prestressed analysis, and output at both surfaces for the element centroidal location. The coarse finite element mesh of the AERO/STAEBL analysis has been found to give quite good static stress results when compared with NASTRAN refined analysis. Figure 8 compares AERO/STAEBL and refined NASTRAN for the chordwise radial stress distributions at the airfoil root.

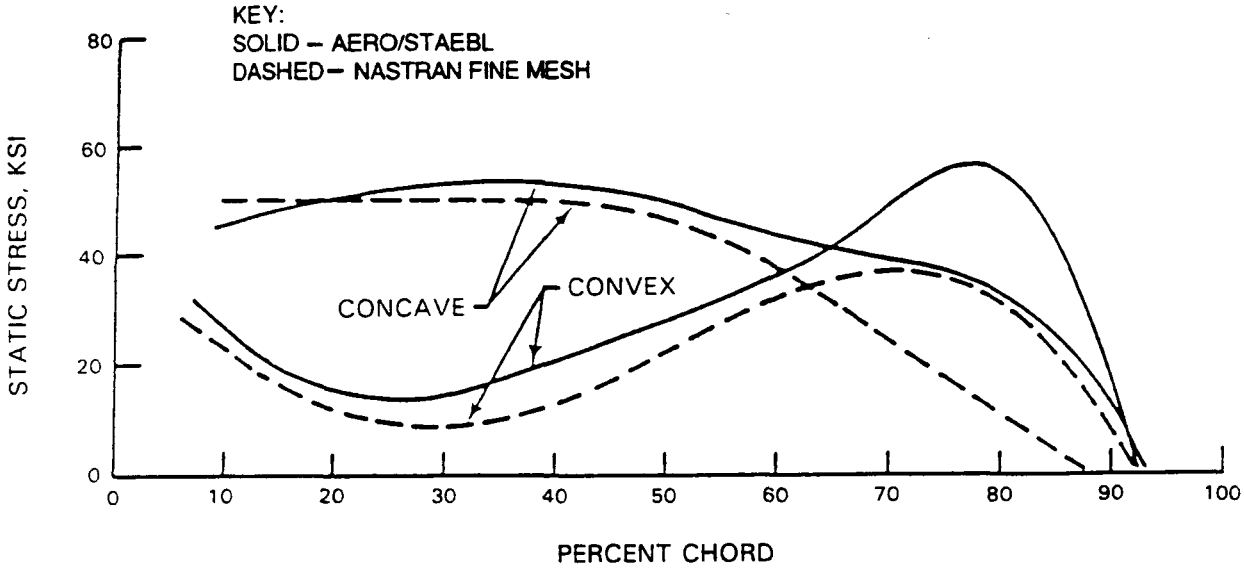

Figure 8 Energy Efficient Engine Fan Airfoil Root Stress

6.3.3 Differential Stiffness

The determination of natural frequencies for rotating blades requires the inclusion of differential stiffness effects. The static displacements are utilized to create the element differential stiffness matrix, which quantifies the element centrifugal stiffening. In addition to differential stiffening, the centrifugal mass matrix, which accounts for the change in direction of centrifugal loads with displacement, is included.

The centrifugal mass matrix (Reference 4), the differential stiffness matrix, and the original blade stiffness are combined to give the blade's total at-speed stiffness. The blade equilibrium equation, after reduction to analysis set size, is solved to find the at-speed blade natural frequencies.

6.3.4 Airfoil Natural Frequencies

The AERO/STAEBL system has shown very good frequency correlations with refined NASTRAN analyses of airfoils. Table VIII shows a frequency comparison for the first three modes for a refined NASTRAN analysis of the Energy Efficient Engine hollow fan and for an AERO/STAEBL representation of the blade. The refined model includes blade ribs and tapered wall thicknesses, which are not modeled in the AERO/STAEBL representation. Hence, much of the discrepancy in the second mode frequency is due to geometric variations in the structural model.

Table VIII

Frequency Analysis Comparison for Energy Efficient Engine Fan

Mode	Refined NASTRAN Analysis (cps)	AERO/STAEBL Analysis (cps)
1	105.6	106.8
2	223.9	266.3
3	299.9	290.5

6.3.5 Postprocessing of Finite Element Output

Static stresses and at-speed eigenvalues, eigenvectors, and nodal stresses are all output from the finite element code. Many of these data must be postprocessed before they may be used either for constraint evaluation or as input to other subroutines. Element stresses must be converted into ply stresses for both static and dynamic modes at elements of stress interest. Additionally, the flutter analyses require both frequency and mode shape information.

The evaluation of static and vibratory composite blade ply stress values requires processing of the element stress values based upon the application of lamination theory. The lamination theory assumes that plane sections (through the plate thickness) remain plane after deformation. The laminate processor provides the matrices required to convert element stresses to element membrane and bending strains. Then, based on the lamination assumptions, ply strains are calculated, leading to ply stresses, and, ultimately, to the Tsai-Wu equivalent stress evaluation.

The evaluation of flutter constraints requires that equivalent beam mode shapes be generated from the available plate mode shape data, due to the beam theory of the present flutter analysis. Beam mode shapes are generated from the available plate mode shapes by performing a spline fit of each component of the mode shape on each cross section. From the spline fit, modal bending and torsional motions are determined at the section shear center, for transmittal to the flutter analysis.

6.4 FLUTTER ANALYSIS

Airfoil flutter consists of a self-excited oscillation of the aerodynamic lifting surface. During the flutter event, the aerodynamic forces of the airstream couple with the blade elastic and inertia forces to increase the energy of the blade. When the level of this negatively damped excitation exceeds the positive damping of the blade material, the blade oscillations will grow to destructive amplitude. Thus, it is imperative that the flutter condition be avoided during engine operation to prevent high frequency fatigue failure of the blade.

In AERO/STAEBL, an available NASA-Lewis flutter code was utilized as the approximate flutter analysis. Using beam-like sectional motions, individual modes of vibration and steady state aerodynamic conditions are input to the analysis. Unsteady aerodynamic loads resulting from vibratory motion are calculated by the aerodynamic analysis. Work done on both the forward and the backward traveling wave for each mode is determined by spanwise integration of the product of resultant unsteady load and input vibratory velocity. Work done is non-dimensionalized by dividing by the kinetic energy of the vibratory mode, resulting in a damping logarithmic decrement. The lowest value of the logarithmic decrement for any mode in any wave direction represents the stage flutter stability measure. In AERO/STAEBL, if this measure is positive, aeroelastic stability is assumed.

The basic assumptions of the flutter analysis are:

- Flow is two-dimensional, unsteady, compressible, inviscid, irrotational, and isentropic
- The cascade is infinite, a flat plate, at zero incidence, and unstalled
- Vibratory motions are small, at constant interblade phase angle, can be represented by two degrees-of-freedom (twist and flap), and occur at the blade/disk system natural frequency.

6.5 FOREIGN OBJECT DAMAGE ANALYSIS

Bird ingestion damage analysis is a nonlinear transient structural dynamics problem which involves fluid-structural interaction, large deflections, and plasticity. A fan blade can fail in the impacted region when the local material strain exceeds material ductility, or away from the impacted region when blade gross deformations due to long-term response result in attachment stresses which exceed maximum strength. Detailed analyses which simulate these responses have been developed, but high computation times prohibit their incorporation into an optimization system. For AERO/STAEBL, accurate simplifications of the detailed analyses have been incorporated within the optimization procedure.

6.5.1 Spanwise Bending Damage

To evaluate the blade gross deformations under impact, a linear, transient, modal analysis is performed. The projectile loading is treated as an impulse acting near the blade tip, at the leading edge. The responses of the blade fundamental modes are tracked through time, and the maximum total stress is noted. Experience has shown that the highest root stresses occur at the quarter cycle of the first bending time point.

6.5.2 Local Damage Analysis

An approximate foreign object damage analysis model has been developed for and installed in AERO/STAEBL that is computationally efficient while preserving the major interactions of the foreign object impact event. The analysis generates incremental loads from user-defined projectile data. The dynamic impact event is simulated through modal transient integration of a linearized target model. Mode shapes used in this process are provided by AERO/STAEBL's finite element analysis, incorporating elements specially modified for the foreign object damage analysis. A maximum average airfoil leading edge strain is then calculated and used in the blade optimization process. The analysis flow is shown in Figure 9.

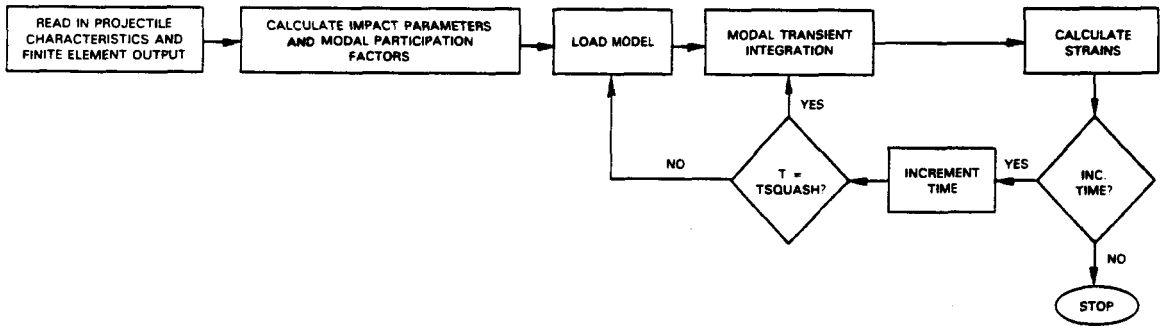

Figure 9 Flowchart of Foreign Object Damage Analysis

The projectile is characterized as a spherical fluid particle with a weight of 1.5 pounds, and a specific gravity of 0.90. The target and the projectile interact during the impact event. A flexible target softens the bird load, but also takes a larger slice of material. The AERO/STAEBL analysis considers these interactions in its loading model.

For purposes of economy, only a local portion of the airfoil is modeled for the local FOD analysis. Within this simply supported leading edge patch, a portion of the elements is assumed to undergo large displacements, and to be in a fully yielded, perfectly plastic state. This assumption results in a linear situation, analogous to the vibrating string problem. By evaluating the natural modes of the approximated structure, a linear modal transient analysis can be performed, ultimately resulting in a leading edge strain history from which the maximum strain is passed to the control module for possible constraint limitation.

6.6 FORCED RESPONSE ANALYSIS

Traditionally, in blade design, high frequency fatigue failure of engine blades is prevented by designing blades to avoid natural frequencies which are coincident with strong excitations at high operating power. A forced response model has been included in AERO/STAEBL which serves as an option to prescribed resonance margins, substituting a study of the blade's forced vibration and steady stress characteristics.

For a given harmonic forcing function distribution, AERO/STAEBL performs a modal forced response analysis to determine the amplitudes of the blade forced vibrations. Once the vibratory amplitudes are determined, AERO/STAEBL combines the steady and vibratory blade stresses using a modified Goodman diagram approach. The worst airfoil stress location on the blade is noted and passed to the optimizer to be used as the working stress constraint.

SECTION 7.0

REFINED ANALYSIS

NASTRAN was selected for use as the refined analysis method for the AERO/STAEBL procedure. It is used regularly to determine steady stresses in solid titanium fan blades for flight cycle life evaluation. A plate element blade model is analyzed in this application. NASTRAN is also used to calculate the vibratory characteristics of composite material fan blades. Equivalent anisotropic material properties are calculated for each finite element using thin laminated plate theory.

Engineering effort in setting up and analyzing solid titanium and composite material blades is minimized through the use of preprocessors and postprocessors. Available processing capabilities include:

- An airfoil preprocessor which generates a NASTRAN plate model of a blade from the airfoil coordinate descriptions
- A laminate preprocessor which calculates the laminate effective stiffness matrices for each finite element and outputs them in a form acceptable to NASTRAN as input data
- A NASTRAN module to calculate laminate strains from the element stresses
- A postprocessor to calculate ply stresses from NASTRAN element stresses.

The flight cycle life and vibratory characteristics of the hollow titanium Energy Efficient Engine fan blade were also evaluated using NASTRAN analysis. In that case, separate models of the concave and convex airfoil walls were employed to verify that a sufficient number of ribs were provided. This made the analysis quite cumbersome and impractical for use in the AERO/STAEBL procedure.

For AERO/STAEBL, it was proposed that hollow blades could be analyzed using a laminated plate model with the central lamina having zero stiffness and density. Re-analysis of the Energy Efficient Engine substantiated this approach. The airfoil breakup was chosen so that the internal ribs are coincident with loci of nodal points. The rib properties are represented by beam elements connecting these nodes. Vibration analysis of the lamination model agrees very well with the more cumbersome original analysis as shown in Figure 10. The breakup in the region of the airfoil root and solid-to-hollow transition was refined, and the centrifugal stresses presented in Figures 11 and 12 were obtained. These stresses are consistent with those predicted by the original design analysis.

The procedure for predicting supersonic flutter of fan stages can evaluate the stability of structural modes which are defined by finite plate element analysis. This ability combines the chordwise bending degree-of-freedom with the flap and twist degrees-of-freedom included in approximate beam blade analysis. The use of the lamination model for blade modal analysis makes it practical to use the expanded flutter prediction procedure for refined analysis. Results of flutter analyses of the Energy Efficient Engine blade are compared in Figure 13. The original design flutter analysis reduced the plate element blade mode shapes to equivalent beam blade modes and concluded that the blade would not flutter under standard operating conditions. The refined analysis supports this conclusion and provides a more accurate technique to evaluate thinner airfoils which are likely to result from structural tailoring.

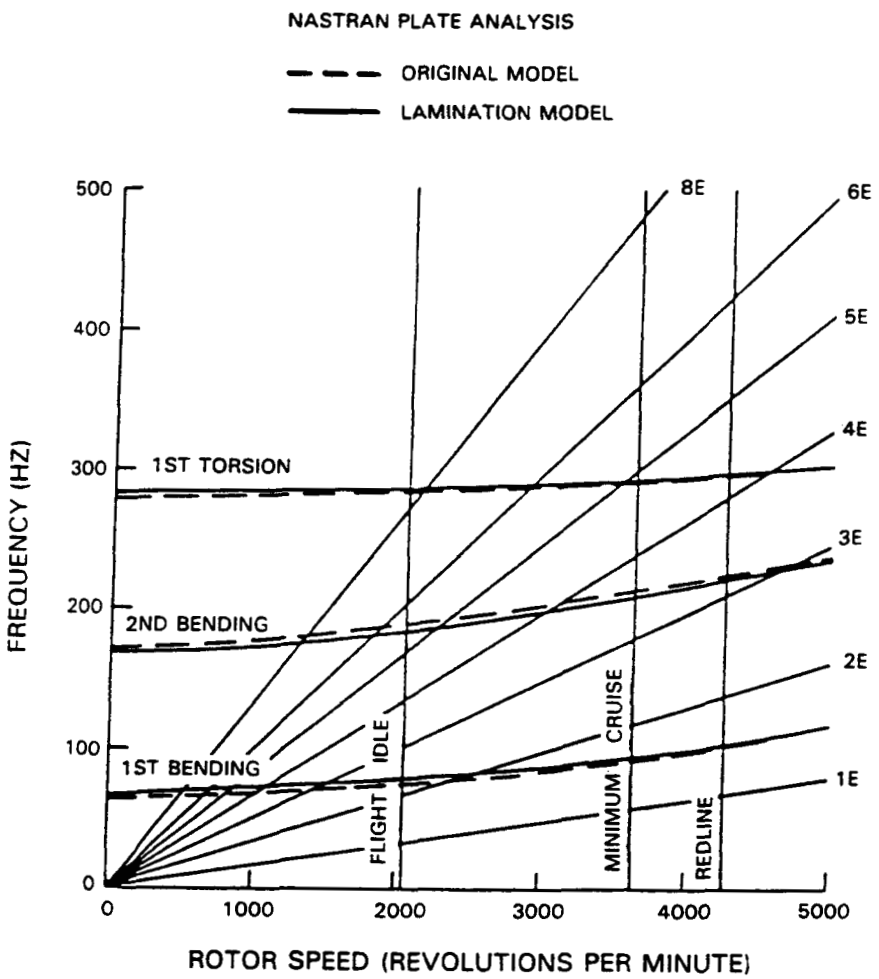

Figure 10 Refined Analysis of the Energy Efficient Engine Hollow Fan Blade

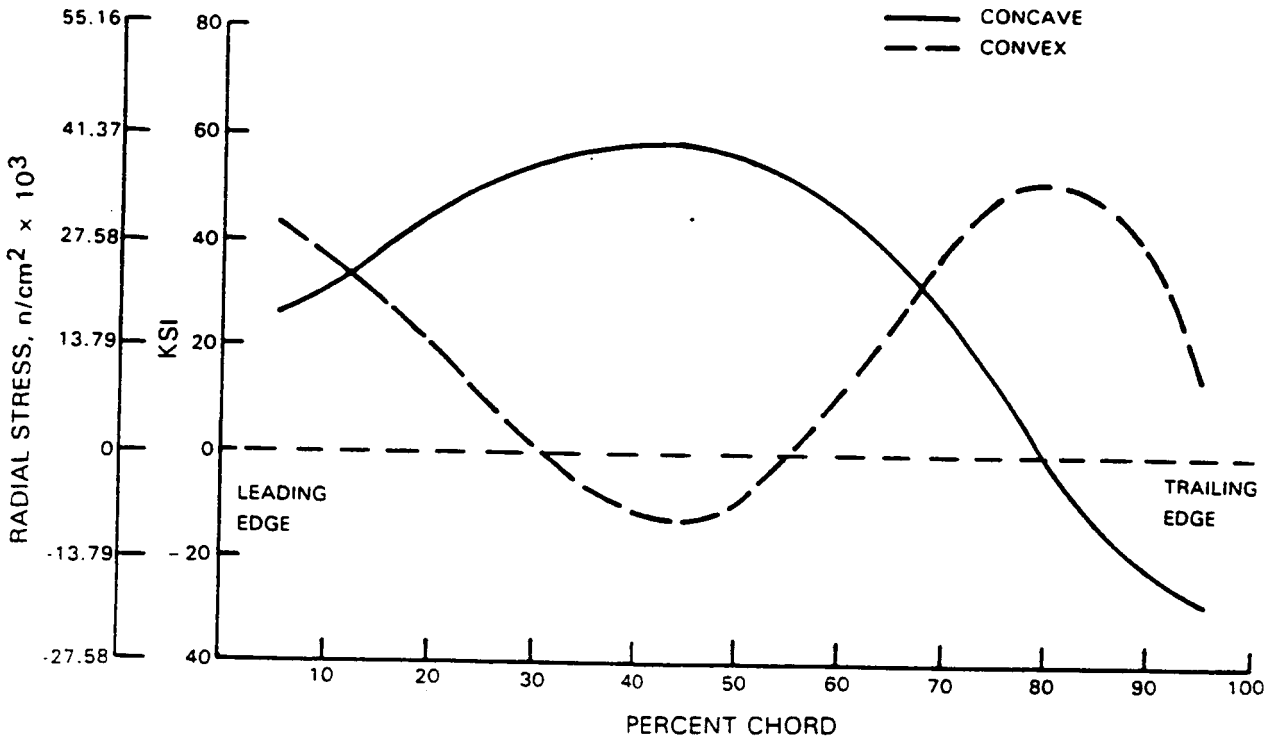

Figure 11 Energy Efficient Engine Hollow Fan Blade Airfoil Root Stress Predicted by Refined Analysis

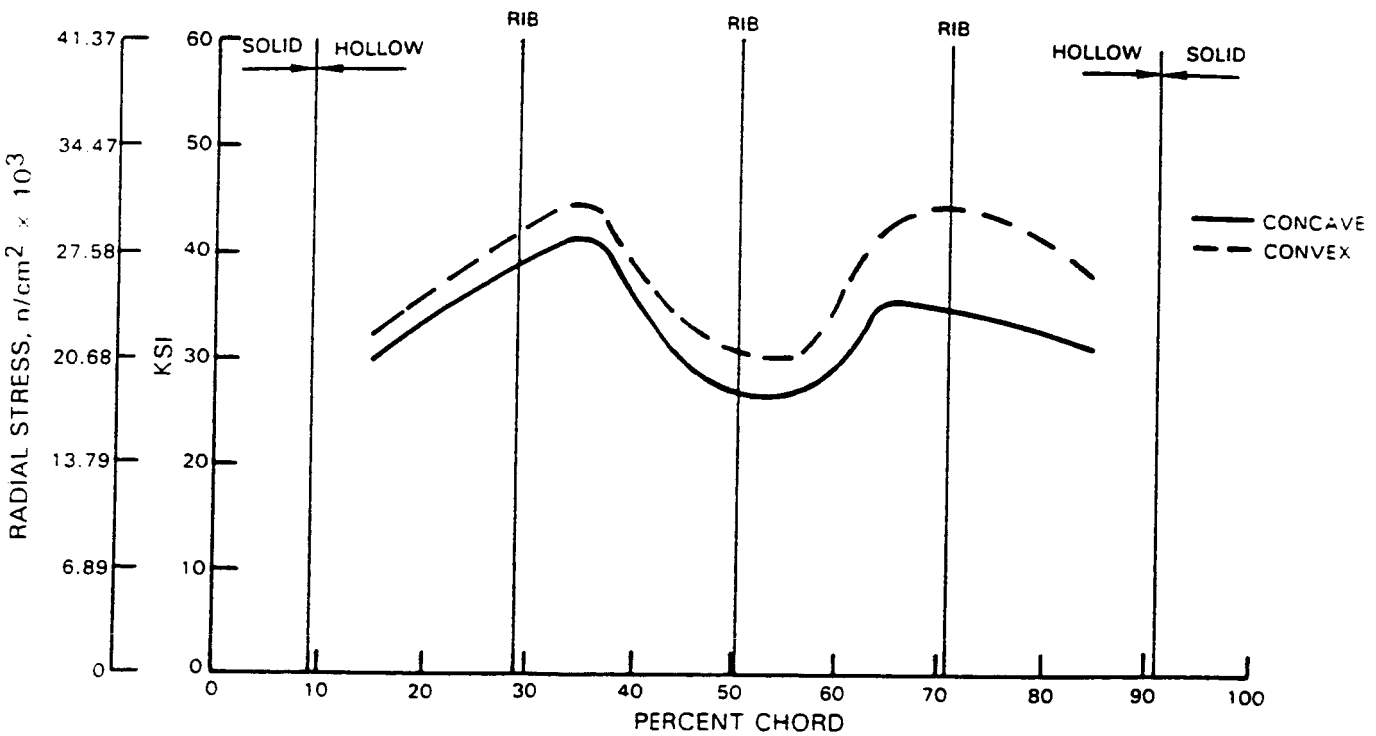

Figure 12 Energy Efficient Engine Hollow Fan Blade Internal Surface Stress at Solid-to-Hollow Transition Predicted by Refined Analysis

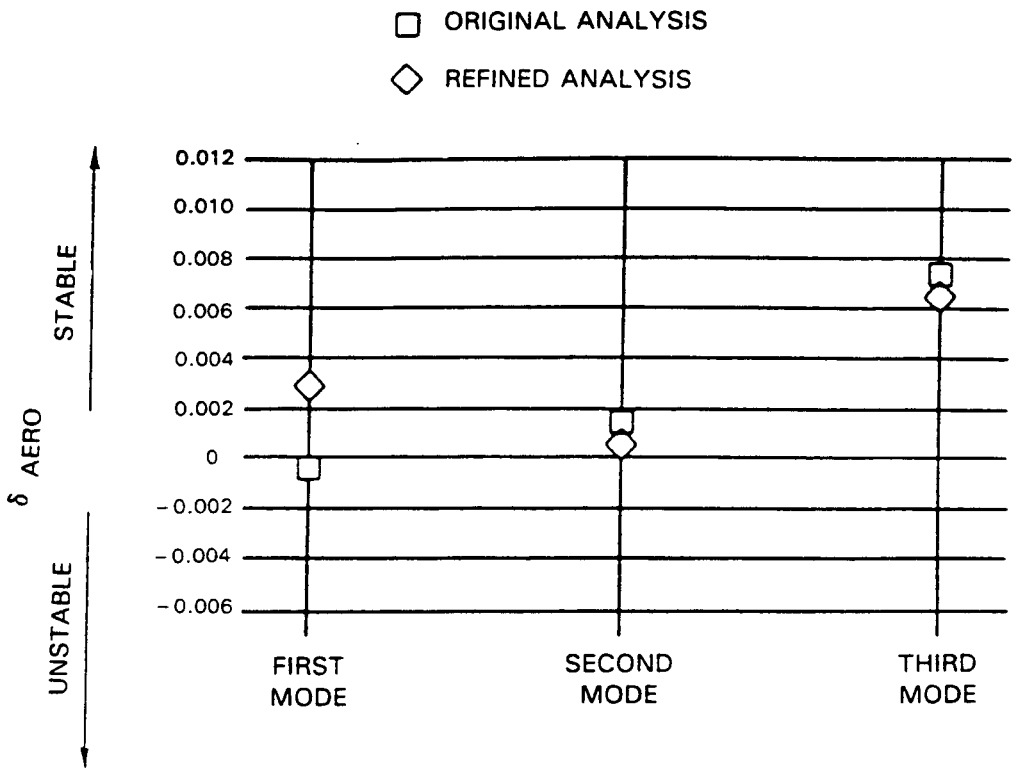

Figure 13 Refined Analysis of the Energy Efficient Engine Hollow Fan Blade Supports the Conclusion that It Would Not Flutter

SECTION 8.0

PROGRAM USAGE

To simplify usage of the AERO/STAEBL program and to reduce the chances for errors in creating optimization cases, many user-friendly features have been added to the AERO/STAEBL system. Input cards are identified by mnemonic titles, and free format inputs are utilized, thus streamlining the date file creation process. A detailed description of the AERO/STAEBL input process is provided in the AERO/STAEBL User's Manual (Reference 5). The general AERO/STAEBL usage concepts are discussed in the following sections.

8.1 DESIGN CURVES

The complete aerodynamic and structural definition of a stage requires the effective processing of many design parameters. In AERO/STAEBL, blade descriptive information is input through design curves, in which blade geometric or aerodynamic parameters are tabulated as functions of an abscissa, in this case the section diameter. These tabulated values are stored as splines, so that a design data base is available, with section information available at any number of stations.

The airfoil geometry is defined through thickness/chord, chord, camber, inlet angle, and edge radius design curves. The leading and trailing edge aerodynamics are defined via design curves that include: air axial locations, relative Mach numbers, air relative and absolute angles, and leading edge static temperature and pressure.

In order to maintain computational effectiveness in AERO/STAEBL, the number of design variables required to produce meaningful design improvements has been minimized by providing for the perturbation of the blade design through a small but select group of design variables. For a given family of airfoil shapes, in this case circular arc airfoils, design perturbations were thus limited to changes in thickness/chord, chord, edge radius, blade count, and relative air inlet angle. Due to the fixed exit aerodynamics, a dependent, or behavior, variable is the camber angle.

By allowing the analyst to select the number of design variables to use in the radial direction for any particular design curve, AERO/STAEBL permits the analyst to tailor the flexibility of the design optimization, while maintaining effective run times. Present experience has shown design tailoring success with up to 20 design variables used.

In AERO/STAEBL, except for a few discrete quantities such as the number of blades, all design data are stored in tabular form as splines of design curves. The design curves are defined in the program as data values with a corresponding abscissa, usually but not necessarily the section radius. The aerodynamic, structural, fabrication and aero/elastic data necessary to describe the blade and its aerodynamic environment are stored in these design tables. Using quintic spline algorithms, design curve reference is available so that any curve may be referenced at any arbitrary required radial location.

8.2 DESIGN VARIABLES

As the design optimization process commences, it is necessary for AERO/STAEBL to update the design curves to reflect the present analysis geometry. Thus, two sets of design curves are maintained: an original set of curves, and a current set. The baseline design curves are updated via design curve increments. A detailed definition of the curve increments is determined via a spline fit of available design variables. Thus, any curve may be updated by having one or more design variables assigned to it. The updated curve is splined, then added to the baseline curve, thus creating the current design curve from which the analysis geometry is derived, as shown in Figure 14.

By using the curve incrementing procedure, several advantages are obtained. First, it is always possible to reproduce a baseline design. If the design variables are the curve values themselves rather than increments, it is difficult to regenerate a baseline geometry without an inordinate number of design variables. By splining increments of baseline curves, a design variable set of zeroes always reproduces the original design. Secondly, the process allows for reducing the optimizer design variable requirements by providing for dependent variables and for constant terms. A dependent variable assignment allows for a curve to be incremented at several abscissa locations even though it may have only one design variable attributed to it. Dependent variables are incremented in user prescribed ratios to the actual design variables, and are unknown to the optimizing algorithm. The provision of a constant variable allows a curve location to be held to a constant value via a prescribed zero increment.

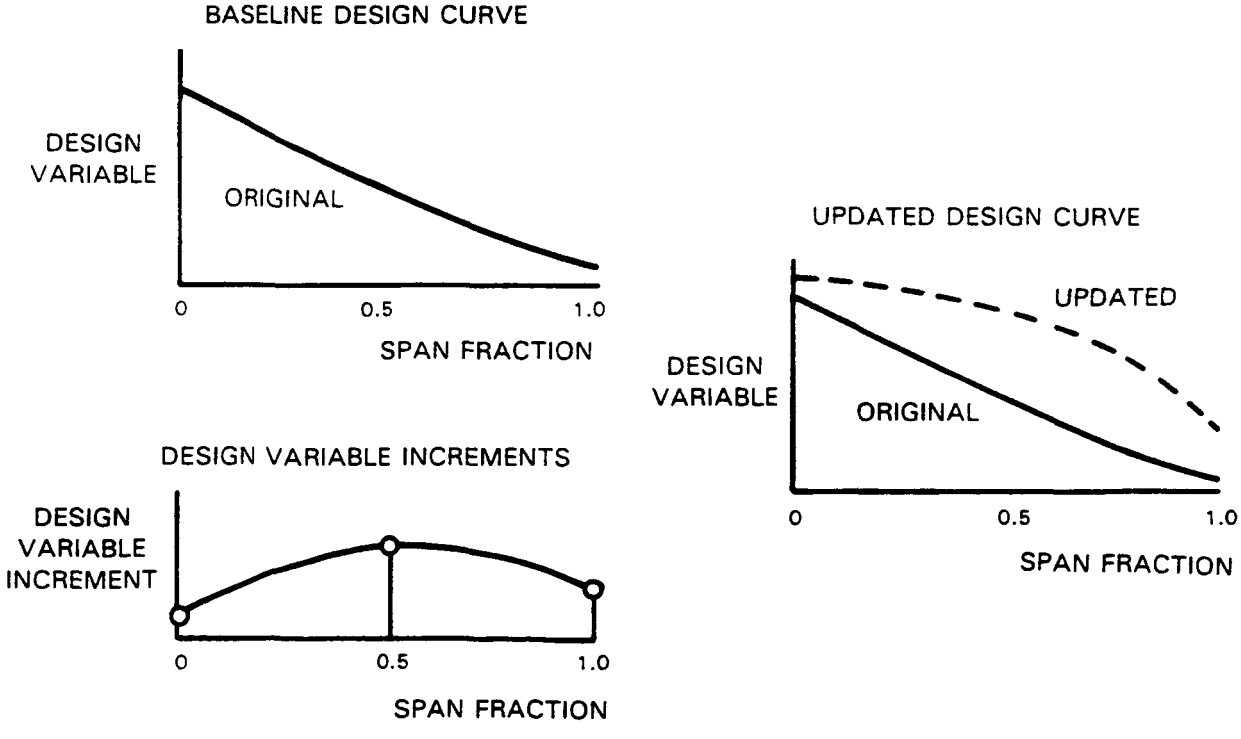

Figure 14 Splined Design Variables Form Curve of Design Increments, Which Update the Baseline Design

8.3 RUNNING POSITION GEOMETRY CORRECTION

Traditionally, aerodynamic design files define the position of the blade in its hot or running position. For shroudless blades, it is usually left to the Structures analyst to define the manufactured, or cold, blade geometry such that at running conditions (including gas, centrifugal and thermal loads) the blade will deflect to the desired geometric position.

Within AERO/STAEBL, the problem of cold geometry determination has been resolved by defining the base blade geometry design curves as representing the cold, rather than the hot, geometry definition. AERO/STAEBL updates the cold geometry to represent the hot geometry for the aerodynamic analyses by incrementing the cold geometry with airfoil deflections as determined from the finite element analysis. The analysis flow for an optimization step, shown on Figure 15, commences with the blade geometry definition. Starting with the cold geometry, an aerodynamic evaluation is performed for the first analysis pass only. This aerodynamic evaluation provides steady state gas loads for the original, cold geometry. While these are not exactly the same loads that the operating blade will encounter, they are a close first approximation and will initiate AERO/STAEBL's geometry iteration process. The geometry generator is now accessed to generate the airfoil coordinates and the finite element mesh. Using the most recent gas loads, a finite element analysis is performed to find the airfoil steady state deflections and stresses and the system natural frequencies. In order to perform an aerodynamic analysis of the proper running position of the airfoil, the aerodynamic geometry curves are updated prior to aerodynamic evaluation, using the static blade deflections predicted by the finite element analysis. The primary curve update is performed on the curve of inlet relative air angles, to account for the effects of blade untwist on the airfoil efficiency. Since the camber is a product of the aerodynamic analysis, no updates are required. Aerodynamic analysis of the hot geometry provides the foil efficiency and updated steady air loads. The blade mesh is now created, and the finite element analysis is performed, thus determining the blade frequencies, stresses, and static deflections.

To provide an exact cold geometry to hot geometry conversion, an iterative process would be required. However, the AERO/STAEBL optimization process is itself an iterative procedure, and early analyses need not have exact geometry corrections. Within AERO/STAEBL, then, the geometry correction process converges as the design converges to its optimum. For the initial analysis pass, air loads on a cold geometry blade are assumed. For subsequent analyses, the gas loads of the previous blade are applied to the finite element analysis of the current geometry to update it to its running position. Since the AERO/STAEBL procedure makes smaller and smaller design changes as the optimization proceeds, the geometry update procedure converges as the design optimization converges. Thus, when the optimization has been completed, both cold and hot blade geometries are available.

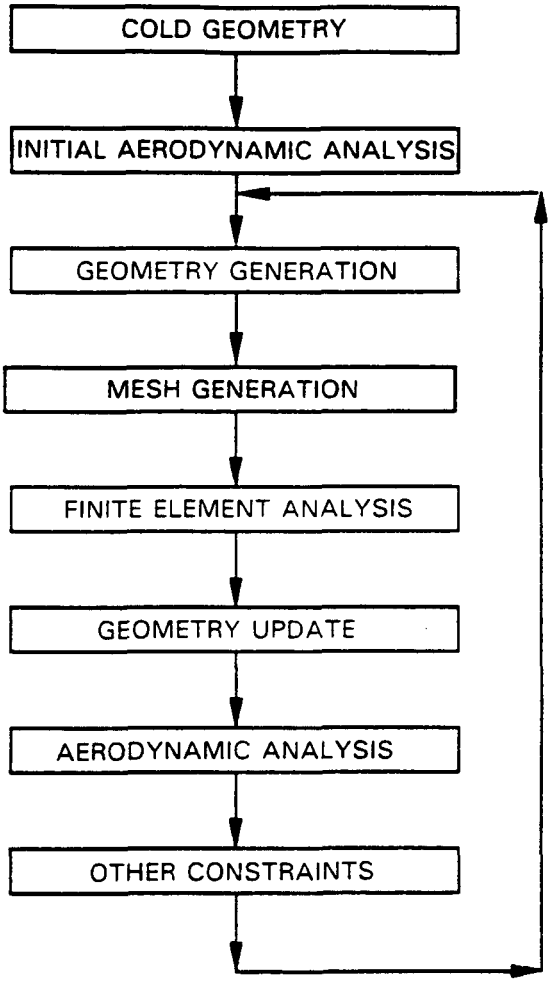

Figure 15 AERO/STAEBL Geometry Update Analysis Flow

SECTION 9.0

VALIDATION CASES

The Energy Efficient Engine has provided the vehicle for the AERO/STAEBL validation cases. Stress, dynamic resonance, and flutter constraints utilized in the design of that engine are directly applicable to the demonstration optimizations of the AERO/STAEBL program. Optimizations have been performed on a solid, sixth-stage compressor blade, and also on two constructions of the hollow fan blade. Initial optimizations were purely structural, with assumptions to maintain the blade aerodynamic performance. Later, aero/structural optimizations were performed, with strikingly different (and improved) results.

With the composite materials used in the demonstration cases, directional strengths vary. Orthotropic material properties are accounted for by use of the Tsai-Wu strength parameter, which is calculated from ratios of stress to strength along orthotropic axes. The parameter yields a single value which is related to the material stress limit, and can be utilized for ingestion - analysis as well as for life cycle evaluations.

For the demonstration cases, the blade resonance constraints often created disjoint feasible regions. In order to increase the probability of determining a global, and not a local, optimum, each structural optimization was preceded by a pre-optimization problem in which resonance constraints had been removed. Each partially tailored design was then final-optimized with all resonance constraints present. Using this sequential optimization process, each of the resultant optimized demonstration blades had resonance characteristics that were similar to those of the respective initial designs, thus indicating that global optimal configurations had been attained.

Details of the validations are presented in the AERO/STAEBL Theoretical Manual (Reference 2). A brief summary of the relevant test cases is provided in the following sections. Table IX shows the reductions in objective function obtained in the structural optimization validations conducted for AERO/STAEBL. In these optimizations, the blade aerodynamics and airfoil efficiency were taken as constant. The objective function was direct operating cost (DOC), except for the optimization of the solid sixth-stage compressor blade, where stage blade weight was minimized.

Table X shows the reductions in objective function obtained in the aero/structural demonstrations of the AERO/STAEBL program. In each case, the objective was to minimize engine direct operating cost. Trade coefficients between fuel cost, material cost, labor cost, and weight represent realistic analysis values, as applied to the Energy Efficient Engine airline economic model.

Table IX

Structurally Tailored Blades

Construction	Objective Function Reduction
Superhybrid Composite Blade	0.039% (DOC)
Hollow Blade with Composite Inlay	0.171% (DOC)
Solid Compressor Blade	30% (Stage Weight)
Superhybrid Composite Blade with Increased Density Patch	0% (DOC)

Table X

Aero/Structurally Tailored Blades

Construction	Objective Function Reduction
Solid Compressor Blade	0.0028% (DOC)
Hollow Blade with Composite Inlay	No Change (DOC)
Superhybrid Composite Blade	0.647% (DOC)

9.1 OBJECTIVE FUNCTION

The procedure used to establish an objective function for the AERO/STAEBL demonstration was modeled after the economic assessment procedure used to guide the design of the Energy Efficient Engine. The Energy Efficient Engine design process was guided by the economic performance assessment of a study airplane defined in the Component Development and Integration Program phase of the contract. The original performance characteristics were updated in 1984 in the study of a large twin airplane in the Energy Efficient Engine Advanced Nacelle Program. The overall airplane characteristics are shown in Table XI. The aircraft is designed for the full specified payload and range, but the economic analysis is conducted for the typical mission payload and range.

Table XI

Energy Efficient Engine Study Airplane Characteristics

	Domestic Trijet
Number of Engines	2
Range - kilometers (nautical miles)	
Design mission	5550 (3000)
Typical mission	1850 (1000)
Passengers	
Design mission	400
Typical mission	55% load factor
Design takeoff gross weight - kilograms (lb)	231,000 (510,000)
Cruise Mach number	0.80
Initial Cruise Altitude - meters (feet)	10,700 (35,000)
Takeoff field length - meters (feet)	2,440 (8,000)

The economic analysis evaluates the effect of changes in engine weight, maintenance cost and first cost against the changes in the aircraft takeoff gross weight and fuel burned to assess the economic effect on the airline. The basis for this analysis is a well developed trade factor technique derived from consideration of airplane aerodynamics, flight mechanisms, propulsion system integration, and weight estimation. The changes in airplane takeoff gross weight reflect a "rubber" airplane analysis, i.e., improvements to the engine configuration will result in further improvements to the airplane configuration. For example, a concept which reduces engine weight will result in a fuel savings which, in turn, further reduces aircraft weight and aircraft structural component weight, permitting reductions in wing size and engine thrust requirements. Consequently, the initial engine weight benefit "snowballs" in its effect on the aircraft benefit.

The life cycle ownership costs determined in this analysis are expressed as direct operating costs plus interest (DOC + I). A trade factor technique derived from considerations of total airline economics provides the basis for this analysis, and includes crew cost, fuel cost, airframe and engine depreciation, airframe and engine maintenance cost, insurance cost, and overhead cost. These trade factors are applied to the specific engine and airplane for which each engine change has been determined. Trade factors for changes in engine weight, maintenance cost, and first cost are applied independently to determine the effect of each engine change on a given economic parameter. Individual effects are then combined to evaluate the total

effect of the advanced concept on that parameter. DOC + I is an extension of DOC in that it includes the "cost of money" (i.e., it includes an expected return to the airline for their investment in the aircraft/engine system). DOC + I is an appropriate substitution for ROI (return on investment) and includes all of the engine related terms in ROI, and is, therefore, an appropriate parameter for evaluating the effect of engine changes on an airline's economics.

The ground rules for the airline economic model are shown in Table XII for the Energy Efficient Engine fan. The 15 percent cost of capital shown is the "interest" in the parameter DOC + I.

Table XII

Energy Efficient Engine Airline Economic Model

- 1983 Dollars
- $0.262/Liter ($1.00/Gallon) Domestic Fuel Cost
- 0.5% Per Year Insurance
- Spares - 5% Airframe, 30% Engine
- Maintenance - Labor Rate = $9.70/Hr, Burden = 200%
- Airline Price - Pratt & Whitney Equation
- Depreciation - 15 Year Straight Line to 10% Residual
- Non-Revenue Flying - 2% Factor on Fuel and Maintenance
- Ground Time - 15 minutes (Domestic)
  - 20 minutes (International)
- Cost of Capital = 15%

The resulting function is:

$$\%\ DOC + I = 0.43\ (\%\ TSFC) + 0.40\ (\ weight\ (lb)\ /\ 1000)$$
$$+ 0.21\ (\ cost\ (\$)\ /\ \$100.000)$$
$$+ 0.32\ (\ maintenance\ cost\ (\$/EFH)\ /\ \$10).$$

By relating the changes in design variables to changes in engine weight, engine manufacturing and maintenance cost, and fuel consumption, AERO/STAEBL is able to provide meaningful DOC + I objective function comparisons for candidate blade designs.

9.1.1 Engine Weight

Individual airfoil weight is an output of the subroutine which generates the element ply layups and equivalent material properties. Total airfoil weight is the product of the individual airfoil weight and the number of blades. Disk and containment case required weights are related to the individual and/or total airfoil weight.

A study was conducted to evaluate these relationships using preliminary design procedures which are regularly applied in estimating engine weight. Three different blade constructions were assumed and blade chord was varied over a range of relevant blade aspect ratios. Individual foil weights and fan system weight were calculated. Cross-plotting the results generated the rather unexpected conclusion that, within engineering accuracy, fan system weight is a simple function of individual airfoil weight. This function is depicted in Figure 16.

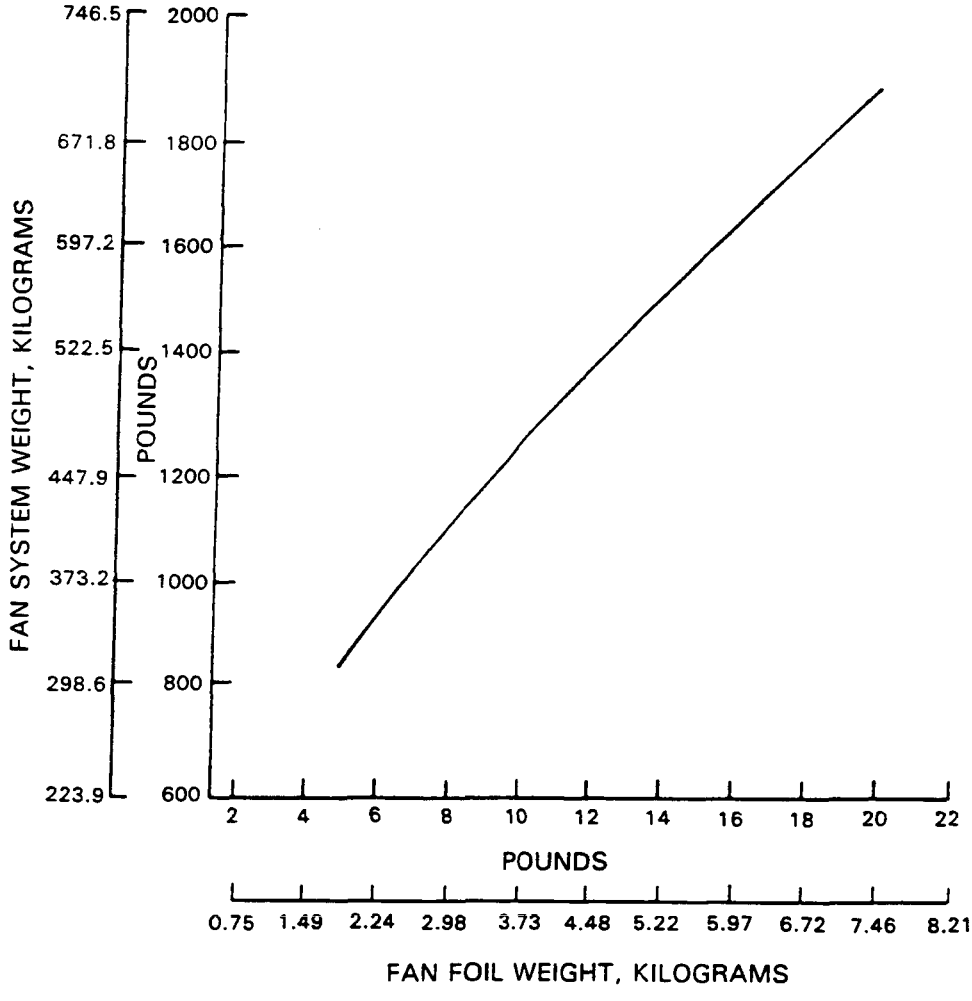

Figure 16 Fan System Weight Is a Simple Function of Individual Airfoil Weight

9.1.2 Engine Cost

Information from Reference 6 was used as a basis for estimating costs of individual fan blades. The hollow blade is made from laminations of titanium and borsic-titanium sheet with hollow cavities produced using leachable iron cores. The stacked laminates are canned, hot isostatically pressed and isothermally forged to shape. The superhybrid blade is made from plies of graphite-epoxy, boron-aluminum, and titanium with adhesive added for metal ply bonding. Stacked plies are vacuum debulked and molded. Materials cost depends on the amount of each component material, which is related to the design variables by the composite blade approximate analysis subroutine. Labor cost depends on blade size as indicated by the design variables root chord and root thickness. Total blade cost is the product of individual blade cost and the number of blades. The change in engine cost for changes in design variables is the change in total blade cost plus an experience-based assessment of costs of related structures which reduces to cost per unit engine length multiplied by change in blade chord.

9.1.3 Maintenance Cost

Engine maintenance histories show that the dominant factor in fan maintenance cost is the number of blades which must be discarded after an ingestion event because they are damaged beyond repair. Service experience provides a definition of the frequency of major ingestion events, the percentage of blades damaged by an event and the solid titanium blade repair/scrap ratio. A hollow blade is expected to have a lower ratio because damage in or near the cavity is not repairable. The controlling parameter is expected to be the design variable distance from the airfoil leading edge to the forward boundary of the cavity. Experience and judgement have been applied to generate the definition, shown in Figure 17, of hollow blade scrap life from known end points. Life is increased in proportion with swept flowpath area when the cavity inner bound is outboard of the airfoil root. Superhybrid blades are assumed to be unrepairable. Total maintenance cost per flight hour is equal to the blade set fabrication cost divided by scrap life.

9.1.4 Fuel Consumption

A review of the engine performance based on the Energy Efficient Engine mission cycle showed that a 1% improvement in fan aerodynamic efficiency results in a 0.6% improvement in engine thrust specific fuel consumption (TSFC). Since the TSFC change is related directly to the DOC + I through the objective function, fan efficiency has now been related to the engine system cost.

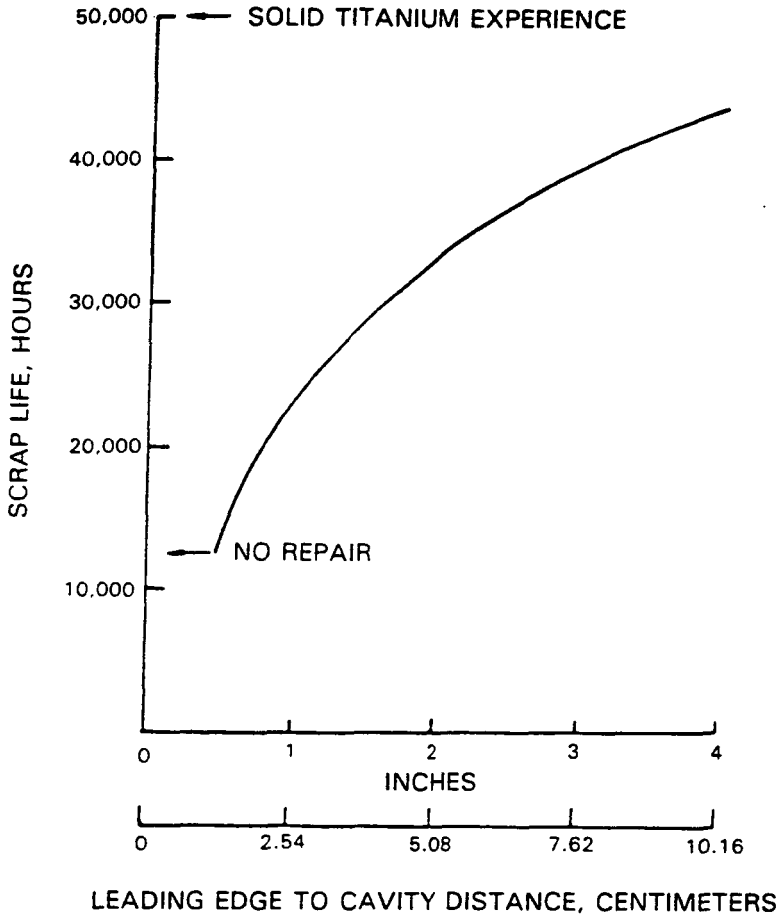

Figure 17 Full Span Hollow Fan Blade Life Is Derived from Solid Blade Experience Limits

9.2 STRUCTURALLY TAILORED BLADES

Four validation cases were performed using the structural tailoring capability of AERO/STAEBL. For these cases, the objective function was engine DOC + I, but with blade efficiency held constant. Within the tailoring, it was assumed that constant efficiency could be maintained by holding blade solidity (gap/chord ratio) constant, and by holding the blade aerodynamic angles constant. (As discussed in Section 9.3, this assumption was later shown to be an oversimplification of the effects of thickness and chord change on blade aerodynamic performance). The validation cases consisted of:

(1) A shroudless, superhybrid composite blade constructed of layers of titanium, graphite epoxy, and boron aluminum

(2) A shroudless, hollow titanium blade using a composite inlay of boron titanium

(3) A solid blade from the sixth stage of the Energy Efficient Engine high-pressure compressor

(4) The shroudless, superhybrid blade of (1) above, but with a patch of variable size and material density at the foreign object damage impact region.

Engine configuration dependent parameters of the Energy Efficient Engine fan component design were held constant while others were allowed to vary. Those parameters that were held constant include: the airflow through the fan component of the Energy Efficient Engine, which is 622.7 kg/sec (1372.8 lbm/sec); the tip speed of 456 m/sec (1496 ft/sec); and the average pressure ratio of 1.7. The hub/tip radius ratio of 0.34, the tip/root chordal taper of 1.46, and associated airfoil stagger and camber angles were also held constant during the structural tailorings.

The basic blade chord was allowed to vary and the number of blades was changed inversely with chord to maintain constant aerodynamic gap/chord ratio at any radial location. The spanwise distribution of airfoil section maximum thickness was allowed to vary, but the ratio of thicknesses at any two fraction of chord positions was held approximately constant. Maximum thickness was never allowed to exceed ten percent of local chord.

For each case, the first refined analysis generated correction factors which were applied to the approximate analysis for reoptimization. The second refined analysis confirmed that design constraints were in fact satisfied.

Two additional superhybrid blade optimizations were made to demonstrate the NASA flutter and forced response options in AERO/STAEBL.

9.2.1 Superhybrid Composite Blade

This test case consisted of the tailoring of a solid fan blade fabricated of superhybrid (titanium, boron/aluminum, graphite/epoxy sandwich) material. Eleven geometric quantities were varied in this demonstration, including chord, thickness, skin thickness, boron composite fraction, and composite material angles.

The first structural tailoring converged on an optimum design after 15 iterations, using 54% boron aluminum (oriented nearly radial by the optimizer). AERO/STAEBL was able to reduce the overall engine direct operating cost (DOC) by 0.003% over the original, hollow fan design. The refined analysis results showed that approximate analysis error had permitted a minor violation of first mode flutter stability.

Due to significant changes in the initial frequency calibration factors, the second tailoring required 19 design iterations before a new optimum could be achieved. AERO/STAEBL was finally able to improve the design by a slight margin over the previous optimum, resulting in a DOC reduction of 0.039% over the original design.

A second refined analysis indicated that the optimized superhybrid design was a valid design and hence was judged to be an acceptable optimum. Additionally, these correlations between the approximate analyses and the refined analysis demonstrated that the dedicated finite element system of AERO/STAEBL performs quite well with respect to required accuracy.

9.2.2 Hollow Blade with Composite Inlay

An alternative construction Energy Efficient Engine fan blade, consisting of a hollow titanium blade with borsic-titanium lining the hollow has been optimized in AERO/STAEBL. For this demonstration, 13 design variables were employed, including blade chord and thickness, cavity extent, and inlay thickness and orientation.

The initial pass at the hollow blade optimization produced interesting results. After three design move steps, AERO/STAEBL was unable to improve on its initial blade design, and optimization was terminated. To determine if this design was a local minimum, another optimization pass was made, but starting with the final hollow blade of a previous optimization pass. After ten iterations, an optimum design was found, representing a savings of 0.077% in engine DOC.

A refined analysis was conducted for the initial optimization pass and it was found that scale factors for the first and second modes were relatively unchanged. Third mode scale factor showed a large change, but fortunately third mode resonance was not an active constraint. As with the superhybrid blade, flutter calibrations revealed that approximate to refined analysis correlations were very good, and only minor adjustments were required for the second optimization pass to satisfy first mode 2E flutter stability.

A second optimization of the hollow blade was made, and a new optimum was achieved in seven iterations, representing a reduction in DOC of 0.171%. A refined analysis of this design showed that several elements near the base of the hollow exhibited effective stresses above the allowable. These values are caused primarily by the presence of relatively high in-plane shear stresses. In a blade, these shear stresses would result in slight local yielding, resulting in load redistribution, without structural damage to the blade. Thus, the second pass optimized hollow blade is judged to be an acceptable design.

9.2.3 Solid Compressor Blade

The high-pressure compressor inlet stage (sixth compressor stage) of the Energy Efficient Engine was also selected for optimization. Design of this blade required that resonance limits be placed on the tip mode frequency for excitations by a tenth harmonic source. A tip mode detection scheme was developed to identify the characteristic mode shape (if within the range of modes evaluated) and use its frequency as a constraint in the optimization process. Six geometric quantities were varied in this demonstration case, including blade chord, and thickness at six radial locations.

The first optimization pass of the solid blade required five iterations but did not employ a flutter constraint. Later, when first pass recalibration calculations were made, flutter stability was found to be violated, and chord length reduction was shown to be excessive. To avoid the flutter instability problem with the next optimization pass, a reduced velocity parameter previously established for the inlet stage of the Energy Efficient Engine was used as a flutter constraint.

When the sixth stage blade was optimized using the AERO/STAEBL system, the blade chord was reduced by nearly 40%. The objective function, blade stage weight, was reduced by nearly 30%.

9.2.4 Superhybrid Blade with Local Increased Density

The final structural optimization validation test case was the superhybrid blade, but with a local patch of increased density. For the AERO/STAEBL tailoring, the local density patch was treated as a no-stiffness add-on to the original element densities. The patch location was defined using five design variables: density, patch distances from the blade root and tip, and distances from the blade leading and trailing edges.

The AERO/STAEBL optimization proceeded for 21 design iterations, until it halted after having found the optimum. The final design of this optimization is very similar to the final superhybrid configuration, although 1.1 pounds of patch material remains in the blade. The final objective function for this design is 0.064% higher than that achieved for the superhybrid blade with no inlay. Therefore, a superior local density configuration would be to completely eliminate the added mass. The optimization scheme of AERO/STAEBL (COPES/CONMIN at the time) apparently finds it difficult to completely eliminate a design variable, although, as in this instance, noticable improvement may develop through that elimination.

9.3 AERO/STRUCTURALLY TAILORED BLADES

To test the aero/structural tailoring capability of AERO/STAEBL, three of the previous structural optimizations were retailored. For these test cases, the objective function remains direct operating cost plus interest, but with blade efficiency effects now included. All blade changes are made such that both upstream and downstream aerodynamics are held constant. Thus, AERO/STAEBL can optimize only a single airfoil row. The validation cases consisted of:

(1) The solid compressor blade from the sixth stage of the Energy Efficient Engine high-pressure compressor

(2) The shroudless, hollow titanium blade with boron titanium inlay

(3) The shroudless, superhybrid composite blade constructed of layers of titanium, graphite epoxy, and boron aluminum.

For each verification test, the initial design was taken as the optimized configuration as determined by the structural optimizations of Section 3.1. For each case, the so-called "optimum" configuration was found to entail large aerodynamic performance penalties, thus demonstrating that weight optimization is second order in importance to performance optimization for total engine cost. Improved results were obtained in each test case by reoptimizing, but starting from the original, bill-of-material blade design.

Each fan verification case was checked by a refined analysis, which revealed minor constraint violations. Correction factors were applied to the AERO/STAEBL approximate analyses, and the optimizations were reconducted. Subsequent refined analysis verifications showed that the superhybrid blade was a valid design optimization. For the hollow blade, a constraint violation was indicated. The hollow blade constraints were readjusted, and a third, and final, optimization was conducted.

These AERO/STAEBL aero/structural optimizations have shown that the addition of aerodynamic degrees-of-freedom are of secondary effect to the blade tailoring, consisting primarily of a fine tuning effect on the dominant variables, thickness and chord. Large differences in final result have been noted, however, by the presence of the aerodynamic efficiency analysis. The previous assumption that a constant gap/chord ratio would maintain rotor efficiency has proven to be incorrect. Those designs previously thought to be optimum have proven to be quite inefficient with the AERO/STAEBL loss calculation included. Thus, with the built-in efficiency calculation, AERO/STAEBL is better prepared to proceed towards a minimum cost engine, rather than just towards a minimum cost blade.

9.3.1 Solid Compressor Blade

The sixth compressor stage of the Energy Efficient Engine has been aero/structurally tailored, using an engine cost objective function. A total of 11 design variables was employed, consisting of five thickness/chord values, blade root chord, number of blades, edge radius, and three values of inlet relative angle. When the optimized blade of Section 9.1.3 was analyzed using the aerodynamic analysis capability of AERO/STAEBL, rotor efficiency was found to drop to 17% from an original 94.3%. Overall, the stage weight reduction had resulted in an engine operating cost increase of 2%. Using the AERO/STAEBL aero/structural tailoring procedure, an optimization was conducted that was able to reduce engine operating cost by 0.0028% for the redesigned stage, which had a rotor efficiency of 94.4%. Most of the cost gain derived from performance benefits gained by reducing blade thickness and edge radius.

9.3.2 Hollow Blade with Composite Inlay

A hollow titanium Energy Efficient Engine fan blade with a borsic titanium inlay in the area of the hollow cavity was also aero/structurally optimized in AERO/STAEBL. Fifteen design variables were utilized in this demonstration. Chord and thickness design variables were present in the same form as was utilized for the superhybrid blade tailoring. Thickness of the titanium shell and of the borsic titanium inlay were considered as design variables. The rectangular cavity chordwise and spanwise extents were defined via four design variables: cavity meanline location, cavity chord width fraction, and upper and lower span fraction radial cutoff locations. Aerodynamic design variables consisted of the blade count, the blade edge radii, and the relative air inlet angles.

When the optimized blade of Section 9.1.2 was analyzed, rotor efficiency was found to be 28.0%, compared with 87.8% for the original, hollow fan design. The previous optimization had resulted in an increase of 5.5% in engine cost, due to the lack of an aerodynamic loss calculation. Using the aero/structural tailoring capability of AERO/STAEBL, an inlaid hollow blade was designed that was able to reduce engine operating cost by 0.26%. Most of the engine cost gains derive from the aerodynamic benefits of thinning the blade tip sections. The efficiency of the optimum airfoil was increased by 0.01%, along with a 0.66 pound blade weight reduction. Little change was noted in the aerodynamic design variables.

Refined analysis of the optimized hollow blade with a borsic-titanium inlay has been conducted using NASTRAN and a refined flutter analysis. A NASTRAN stress analysis, postprocessed to determine lamina stresses, showed that all Tsai-Wu values were below 0.25, and hence all stresses are acceptable. Refined frequency results showed very good correlations with the AERO/STAEBL approximate analyses.

Reviewing the blade resonances, based upon the refined NASTRAN analysis, it was found that second mode 4E and also third mode 4E resonance constraints are violated by the first pass optimized blade. Refined flutter analysis for the optimized blade showed no flutter constraint violations.

By adjusting the frequency correction factors on the resonance constraint cards, the analyses were recalibrated. An optimization was conducted, starting from the latest optimized geometry. AERO/STAEBL, after considerable effort, was able to locate a feasible blade with the new calibration factors included. From this previously optimum starting point, however, an engine cost penalty of 13.46% was incurred in locating this locally optimal blade. More encouraging results were obtained by reoptimizing, but starting with the original Energy Efficient Engine fan geometry. This new optimal design enables an engine cost savings of 0.212%. Blade efficiency has been increased from 87.76% to 88.55%.

A refined analysis of this recalibrated, reoptimized blade has been conducted. NASTRAN stress analysis indicates a maximum Tsai-Wu value of 0.90 in the titanium, in the solid root section, indicating that all stresses are acceptable. Frequency recalibrations showed a change in the third mode calibration factor. This accuracy deterioration results in a 4% violation of the third mode 4E resonance constraint. Refined flutter analyses have shown that all modes of this optimized blade are acceptable for both forward and backward travelling waves.

The approximate analyses were recalibrated, and a third optimization was attempted, starting from the final design of the previous optimization. Due to the unexpected 4% drop in third mode frequency correction factor, the previous optimum is now an infeasible design, and adjustments to the blade will be required. AERO/STAEBL was unsuccessful in reoptimizing the hollow blade design, being unable to sufficiently separate the second and third mode frequencies to pass frequency margin requirements.

To provide more design flexibility for AERO/STAEBL, two more thickness design variables were included in the optimization, namely blade thickness at the 25% and the 75% span locations. Additionally, at this time the capability for static gas loads was added to the AERO/STAEBL aerodynamic analysis. To compensate for the bending stresses caused by the aerodynamic loadings, tilt variables have also been added to the AERO/STAEBL system. The tilt of the blade section is the distance (either axially or tangentially) between the section center of gravity and the airfoil radial stacking line. If no tilt curves are defined, the section tilt is taken to be zero, and gas load effects are ignored. With tilt curves defined, gas loads are included, and tilt design variables may be defined in the normal manner by which variables are assigned to designated design curves in AERO/STAEBL.

To investigate the effects of adding gas loads and tilt variables to the inlaid hollow fan blade, an optimization commencing at the final design of the previous tailoring was initiated. For this optimization, two stacking design variables were included: axial tilt at the blade tip, and tangential tilt at the blade tip. By enforcing tilt values of 0.0 at the blade root, and assigning midspan tilts to be half of the tip tilts through dependent variable designations, linear tilts were enforced on this optimization case. These linear tilts were deemed adequate for testing the tilt option of AERO/STAEBL, for the primary purpose in tilting a blade is to negate gas bending stresses. Experience has shown that root stress cancellation can be fully attained using a tilt that varies linearly from root to tip. As with the previous optimization attempt, AERO/STAEBL was unsuccessful in finding a feasible design, being unable to sufficiently separate the second and third mode frequencies of the hollow blade.

9.3.3 Superhybrid Composite Blade

The Energy Efficient Engine fan blade was tailored for a superhybrid construction, consisting of a boron aluminum core, covered by a section of graphite epoxy, and with a titanium shell and titanium center ply. The tailoring process was executed with 14 design variables. The blade thickness/chord ratio was allowed to vary at three spanwise locations. The

blade root chord was a variable, with the chords at other blade sections varying in proportion with root chord variations. The blade was sheathed with a uniform thickness titanium skin, with skin thickness a design variable. The thickness of the uniform central titanium ply was allowed to vary. The balance of the blade representation consisted of a boron aluminum layer of variable thickness and material angle. The remainder of the blade consisted of graphite epoxy with a variable material angle. Aerodynamic design variables consisted of the blade count, the blade edge radii, and the relative air inlet angles.

When the optimized blade of Section 9.1.1 was analyzed, rotor efficiency was found to be 66.2%, compared with 87.8% for the original, hollow fan design. The previous optimization had resulted in an actual increase of 15.4% in engine cost, due to the lack of an aerodynamic loss calculation. Using the aero/structural tailoring capability of AERO/STAEBL, a superhybrid blade was designed that was able to reduce engine operating cost by 0.34%. Most of the engine cost gains derive from the aerodynamic benefits of thinning the blade tip sections. The efficiency of the optimum airfoil was increased by 1.4%, along with a 0.9 pound blade weight reduction. Little change was noted in the aerodynamic design variables, although there was a slight increase in the blade edge radius, presumably to maintain local foreign object damage resistance.

Refined analyses have been conducted on the optimized superhybrid composite fan. A NASTRAN stress analysis showed unacceptable stresses in the outermost root boron/aluminum plies. NASTRAN frequency calibrations, while very good, showed a 3% margin violation for the third mode 4E resonance condition.

The constraints for this optimization test case were modified, and the analysis was restarted from this latest optimum configuration. AERO/STAEBL was very successful at fine tuning the superhybrid blade design, not only achieving a feasible blade, but simultaneously reducing the DOC + I by another 0.29%. The efficiency of the final design is 90.3%, representing the best blade which AERO/STAEBL has found to date.

Subsequent to the optimization of the recalibrated superhybrid blade design, gas loads were added to the aerodynamic analysis. To compensate for the bending stresses caused by the aerodynamic loadings, tilt variables have also been added to the AERO/STAEBL system.

To investigate the effects of adding gas loads and tilt variables on the optimized superhybrid fan blade, an optimization commencing at the final design of the previous tailoring was initiated. After 27 function evaluations, AERO/STAEBL halted the optimization run, with no change to the optimum design. Since stress is not an active constraining parameter for the optimized superhybrid blade, tilting of the blade is not a requirement. Since tilt adds no improvement to the blade's aerodynamic performance, AERO/STAEBL has no motivation to change the design from that derived without considering tilt effects.

SECTION 10.0

CONCLUSIONS AND RECOMMENDATIONS

The AERO/STAEBL program has successfully applied mathematical optimization procedures to shroudless fan and compressor blade structural tailoring, and has shown it to be a very powerful automated design procedure. STAEBL's design optimization procedure provides the capacity to simultaneously evaluate the effect of changes to many design variables to minimize a comprehensive objective function while observing numerous design constraints. The blade design applications of this study are relatively novel because of the preponderance of dynamic design constraints which, since critical excitations can be avoided by making structural frequencies higher or lower, create the possibility of disjoint feasible regions. In the AERO/STAEBL demonstrations to date, however, this possibility of local frequency induced optima has not been noted to limit the system's potential for improving a design or finding a feasible design where none is known to exist.

The composite blade tailoring applications have demonstrated the capability of the AERO/STAEBL procedure to select appropriate values for a large number of design variables due to the flexibilities provided by the complicated internal constructions which could be changed in many ways without affecting aerodynamic performance. Checkout studies have also demonstrated that the AERO/STAEBL optimization procedure is a useful tool for tailoring of blades fabricated from homogeneous material. The various natural modes of blade vibration have proven to be sensitive to the spanwise distribution of airfoil thickness to a level of refinement that can only be defined by several variables. Even the most experienced design analyst would only be able to find an approximation to the best distribution, and even then at a much greater expense than would be entailed by employing the AERO/STAEBL procedure.

Recent aero/structural optimizations performed by AERO/STAEBL have demonstrated the importance of including aerodynamic efficiency effects in blade optimization. While aerodynamic design variables (edge radius, inlet air angle) have proven to be of secondary importance, the effects of structural design variables (thickness, chord) on blade performance have proven to be quite strong.

Due to the proven capability of AERO/STAEBL to handle difficult optimizations entailing many design variables, it is recommended that the AERO/STAEBL program be expanded to include numerical optimizations of the highly complicated geometries of hollow, cooled turbine blades and vanes. Design of cooling flows and cooling passages is currently a highly detailed, iterative process including much engineer interaction. Application of the AERO/STAEBL optimizer would show dramatic savings in manpower in the turbine blade and vane design process.

REFERENCES

1. Vanderplaats, G. N., H. Sugimoto and C. M. Sprague, "ADS-1: A New General Purpose Optimization Program," AIAA 24th Structures, Structural Dynamics and Materials Conference, Lake Tahoe, Nev., May, 1983.

2. Brown, K. W., "The Aero/Structural Tailoring of Engine Blades (AERO/STAEBL) Theoretical Manual," Pratt & Whitney Report PWA-5774-76, October, 1986.

3. MacNeal, R. H., ed., "The NASTRAN Theoretical Manual," NASA SP-221 (01), April, 1972.

4. Dokainish, M. A. and S. Rawtani, "Pseudo-Static Deformation and Frequencies of Rotating Turbomachinery Blades," AIAA Journal, Vol. 10, No. 11, November, 1972, pp. 1397-1398.

5. Brown, K. W., "The Aero/Structural Tailoring of Engine Blades (AERO/STAEBL) User's Manual," Pratt & Whitney Report PWA-5774-75, October, 1986.

6. Stelson, T. S. and C. F. Barth, "Cost Analysis of Composite Fan Blade Manufacturing Processes," NASA Report CR-159876.

DISTRIBUTION LIST

NASA-Lewis Research Center
Attn: George Virosteck, MS 500-313
21000 Brookpark Road
Cleveland, OH 44135

NASA-Lewis Research Center
Attn: Tech Rept Control Office, MS 60-1
21000 Brookpark Road
Cleveland, OH 44135

NASA-Lewis Research Center
Attn: Tech Utilization Office, MS 7-3
21000 Brookpark Road
Cleveland, OH 44135

NASA-Lewis Research Center
Attn: Contract File, MS 49-6 (2 copies)
21000 Brookpark Road
Cleveland, OH 44135

NASA-Lewis Research Center
Attn: Library, MS 60-3
21000 Brookpark Road
Cleveland, OH 44135

NASA-Lewis Research Center
Attn: L. Berke, MS 49-6
21000 Brookpark Road
Cleveland, OH 44135

NASA-Lewis Research Center
Attn: R. H. Johns, MS 49-8
21000 Brookpark Road
Cleveland, OH 44135

NASA-Lewis Research Center
Attn: L. J. Kiraly, MS 23-2
21000 Brookpark Road
Cleveland, OH 44135

NASA-Lewis Research Center
Attn: C. C. Chamis, MS 49-6 (5 copies)
21000 Brookpark Road
Cleveland, OH 44135

NASA-Lewis Research Center
Attn: M. S. Hirschbein, MS 49-8
21000 Brookpark Road
Cleveland, OH 44135

NASA-Lewis Research Center
Attn: J. A. Ziemianski, MS 86-1
21000 Brookpark Road
Cleveland, OH 44135

NASA-Lewis Research Center
Attn: P. B. Burstadt, MS 100-5
21000 Brookpark Road
Cleveland, OH 44135

NASA-Lewis Research Center
Attn: K. R. Kaza, MS 23-2
21000 Brookpark Road
Cleveland, OH 44135

NASA-Lewis Research Center
Attn: R. E. Kielb, MS 23-2
21000 Brookpark Road
Cleveland, OH 44135

NASA-Lewis Research Center
Attn: J. J. Adamczyk, MS 5-9
21000 Brookpark Road
Cleveland, OH 44135

NASA-Lewis Research Center
Attn: R. D. Hager, MS 86-7
21000 Brookpark Road
Cleveland, OH 44135

NASA-Lewis Research Center
Attn: L. J. Bober, MS 86-7
21000 Brookpark Road
Cleveland, OH 44135

National Aeronautics and
Space Administration
Attn: NHS-22/Library
Washington, D.C. 20546

National Aeronautics and
Space Administration
Attn: RTM-6/S. L. Venneri
Washington, D.C. 20546

National Aeronautics and
Space Administration
Attn: R/M. S. Hirschbein
Washington, D.C. 20546

DISTRIBUTION LIST (continued)

NASA Ames Research Center
Attn: Library, MS 202-3
Moffett Field, CA 94035

NASA Goddard Space Flight Center
Attn: 252/Library
Greenbelt, MD 20771

NASA John F. Kennedy Space Center
Attn: Library, MS AD-CSO-1
Kennedy Space Center, FL 32931

NASA Langley Research Center
Attn: Library, MS 185
Hampton, VA 23665

NASA Langley Research Center
Attn: M. F. Card, MS 244
Hampton, VA 23665

NASA Langley Research Center
Attn: W. J. Strout
Hampton, VA 23665

NASA L. B. Johnson Space Center
Attn: JM6/Library
Houston, TX 77001

NASA George C. Marshall Space
Flight Center
Attn: AS61/Library
Marshall Space Flt. Center, AL 35812

NASA George C. Marshall Space
Flight Center
Attn: R. S. Ryan
Marshall Space Flt. Center, AL 35812

Jet Propulsion Laboratory
Attn: Library
4800 Oak Grove Drive
Pasadena, CA 91103

Jet Propulsion Laboratory
Attn: B. Wada
4800 Oak Grove Drive
Pasadena, CA 91103

Jet Propulsion Laboratory
Attn: R. Levi
4800 Oak Grove Drive
Pasadena, CA 91103

NASA S&T Information Facility
Attn: Acquisition Dept. (10 copies)
P. O. Box 8757
Balt.-Washington Int. Airport, MD 21240

Air Force Aero. Propulsion Lab.
Attn: Z. Gershon
Wright-Patterson AFB, OH 45433

Air Force Aero. Propulsion Lab.
Attn: N. Khot
Wright-Patterson AFB, OH 45433

Air Force Systems Command
Aeronautical Systems Division
Attn: Library
Wright-Patterson AFB, OH 45433

Air Force Systems Command
Aeronautical Systems Division
Attn: C. W. Cowie
Wright-Patterson AFB, OH 45433

Air Force Systems Command
Aeronautical Systems Division
Attn: J. McBane
Wright-Patterson AFB, OH 45433

Aerospace Corporation
Attn: Library-Documents
2400 E. El Segundo Blvd.
Los Angeles, CA 90045

Air Force Office of Scientific Res.
Attn: A. K. Amos
Washington, D.C. 20333

Department of the Army
U. S. Army Material Command
Attn: AMCRD-RC
Washington, D.C. 20315

DISTRIBUTION LIST (continued)

U. S. Army Ballistics Research Lab.
Attn: Dr. Donald F. Haskell
MS DRXBR-BM
Aberdeen Proving Ground, MD 21005

Mechanics Research Laboratory
Army Materials & Mechanics Res. Center
Attn: Dr. Donald W. Oplinger
Watertown, MA 02172

U. S. Army Missile Command
Redstone Scientific Info. Center
Attn: Document Section
Redstone Arsenal, AL 35808

AFFDL/FBE
Attn: D. W. Smith
Wright-Patterson AFB, OH 45433

Commanding Officer
U. S. Army Research Office (Durham)
Attn: Library
Box CM, Duke Station
Durham, NC 27706

Bureau of Naval Weapons
Department of the Navy
Attn: RRRE-6
Washington, D.C. 20360

Commander, U. S. Naval Ordnance Lab.
White Oak
Attn: Library
Silver Springs, MD 20910

Director, Code 6180
U. S. Naval Research Laboratory
Attn: Library
Washington, D.C. 20390

Denver Federal Center
U. S. Bureau of Reclamation
Attn: P. M. Lorenz
P. O. Box 25007
Denver, CO 80225

Naval Air Propulsion Test Center
Aeronautical Engine Department
Attn: Mr. James Salvino
Trenton, NJ 08628

Naval Air Propulsion Test Center
Aeronautical Engine Department
Attn: Mr. Robert DeLucia
Trenton, NJ 08628

FAA, Code ANE-214, Propulsion Sect.
Attn: Mr. Robert Berman
12 New England Executive Park
Burlington, MA 01803

FAA, ARD-520
Attn: Commander John J. Shea
2100 Second Street, SW
Washington, D.C. 20591

Rensselaer Polytechnic Institute
Attn: R. Loewy
Troy, NY 12181

Federal Aviation Administration DOT
Office of Aviation Safety, FOB 10A
Attn: Mr. John H. Enders
800 Independence Avenue, S.W.
Washington, D.C. 20591

National Transportation Safety Board
Attn: Edward P. Wizniak, MS TE-20
800 Independence Avenue, S.W.
Washington, D.C. 20594

Arizona State University
Dept. of Aero. Eng. & Eng. Science
Attn: H. D. Nelson
Tempe, AZ 85281

Rockwell International Corporation
Attn: J. Gausselin, MS D422/402 AB71
Los Angeles International Airport
Los Angeles, CA 90009

Cleveland State University
Department of Civil Engineering
Attn: P. Bellini
Cleveland, OH 44115

Massachusetts Institute of Technology
Attn: F. McGarry
Cambridge, MA 02139

DISTRIBUTION LIST (continued)

Massachusetts Institute of Technology
Attn: T. H. Pian
Cambridge, MA 02139

Massachusetts Institute of Technology
Attn: J. Mar
Cambridge, MA 02139

Massachusetts Institute of Technology
Attn: E. A. Witmer
Cambridge, MA 02139

Massachusetts Institute of Technology
Attn: J. Dugundji
Cambridge, MA 02139

Univ. of Illinois at Chicago Center
Department of Materials Engineering
Attn: Dr. Robert L. Spilker
Box 4348
Chicago, IL 60680

Detroit Diesel Allison
General Motors Corporation
Attn: Mr. William Springer
Speed Code T3, Box 894
Indianapolis, IN 46206

General Motors Corporation
Attn: R. J. Trippet
Warren, MI 48090

AVCO Lycoming Division
Attn: Mr. Herbert Kaehler
550 South Main Street
Stratford, CT 06497

Beech Aircraft Corporation
Plant 1
Attn: Mr. M. K. O'Connor
Wichita, KA 67201

Bell Aerospace
Attn: S. Gallin
P. O. Box 1
Buffalo, NY 14240

Boeing Aerospace Company
Impact Mechanics Lab
Attn: Dr. R. J. Bristow
P. O. Box 3999
Seattle, WA 98124

Boeing Commercial Airplane Company
Attn: Dr. Ralph B. McCormick
P. O. Box 3707
Seattle, WA 98124

Boeing Commercial Airplane Company
Attn: Mr. David T. Powell, MS 73-01
P. O. Box 3707
Seattle, WA 98124

Boeing Commercial Airplane Company
Attn: Dr. John H. Gerstle
P. O. Box 3707
Seattle, WA 98124

McDonnell Douglas Aircraft Corp.
Attn: Library
P. O. Box 516
Lambert Field, MO 63166

Boeing Company
Attn: Library
Wichita, KA 67201

Douglas Aircraft Company
Attn: M. A. O'Connor, Jr., MS 36-41
3855 Lakewood Blvd.
Long Beach, CA 90846

Garrett AiResearch Manufacturing Co.
Attn: L. A. Matsch
111 S. 34th Street
P. O. Box 5217
Phoenix, AZ 85010

R. Stockton
Garrett Turbine Engine Company
Rotor Integuity, 503-42
111 S. 34th Street
P. O. Box 5217
Phoenix, AZ 85010

DISTRIBUTION LIST (continued)

General Dynamics
Attn: Library
P. O. Box 748
Fort Worth, TX 76101

General Dynamics/Convair Aerospace
Attn: Library
P. O. Box 1128
San Diego, CA 92112

General Electric Company
Attn: Dr. L. Beitch, MS K221
Interstate 75, Bldg. 500
Cincinnati, OH 45215

General Electric Company
Attn: Dr. R. L. McKnight, MS K221
Interstate 75, Bldg. 500
Cincinnati, OH 45215

General Electric Company
Attn: Dr. V. Gallardo, MS K221
Interstate 75, Bldg. 500
Cincinnati, OH 45215

General Electric Company
Aircraft Engine Group
Attn: Mr. Herbert Garten
Lynn, MA 01902

Grumman Aircraft Engineering Corp.
Attn: Library
Bethpage, Long Island, NY 11714

Grumman Aircraft Engineering Corp.
Attn: H. A. Armen
Bethpage, Long Island, NY 11714

IIT Research Institute
Technology Center
Attn: Library
Chicago, IL 60616

Lockheed California Company
Attn: Mr. D. T. Pland
P. O. Box 551
Dept. 73-31, Bldg. 90, PL. A-1
Burbank, CA 91520

Lockheed California Company
Attn: Mr. Jack E. Wignot
P. O. Box 551
Dept. 75-71, Bldg. 63, PL. A-1
Burbank, CA 91520

Northrop Space Laboratories
Attn: Library
3401 West Broadway
Hawthorne, CA 90250

North American Rockwell, Inc.
Rocketdyne Division
Attn: Library, Dept. 596-306
6633 Canoga Avenue
Canoga Park, CA 91304

North American Rockwell, Inc.
Rocketdyne Division
Attn: J. F. Newell
6633 Canoga Avenue
Canoga Park, CA 91304

North American Rockwell, Inc.
Space & Information Systems Div.
Attn: Library
12214 Lakewood Blvd.
Downey, CA 90241

Norton Company, Indus. Ceramics Div.
Armore & Spectramic Products
Attn: George E. Buron
Worcester, MA 01606

Norton Company, Indus. Ceramics Div.
Attn: Mr. Paul B. Gardner
1 New Bond Street
Worcester, MA 01606

UTC/Pratt & Whitney
Attn: Library, MS 732-11
P. O. Box B2691
West Palm Beach, FL 33402

UTC/Pratt & Whitney
Attn: R. A. Marmol, MS 713-39
P. O. Box B2691
West Palm Beach, FL 33402

DISTRIBUTION LIST (continued)

UTC/Pratt & Whitney
Attn: Library, MS 169-31
400 Main Street
East Hartford, CT 06108

UTC/Pratt & Whitney
Attn: Dr. E. Todd, MS 163-09
400 Main Street
East Hartford, CT 06108

UTC/Pratt & Whitney
Attn: D. H. Hibner, MS 163-09
400 Main Street
East Hartford, CT 06108

United Technologies Corporation
Hamilton Standard
Attn: Dr. G. P. Towsend
Windsor Locks, CT 06096

United Technologies Corporation
Hamilton Standard
Attn: Dr. R. A. Cornell
Windsor Locks, CT 06096

Aeronautical Research Association
of Princeton, Inc.
Attn: Dr. Thomas McDonough
P. O. Box 2229
Princeton, NJ 08540

Republic Aviation
Fairchild Hiller Corporation
Attn: Library
Farmington, Long Island, NY

Rohr Industries
Attn: Mr. John Meaney
Foot of H Street
Chula Vista, CA 92010

TWA Inc., Kansas City Int'l Airport
Attn: Mr. John J. Morelli
P. O. Box 20126
Kansas City, MO 64195

Stevens Institute of Technology
Attn: F. Sisto
Castle Point Station
Hoboken, NJ 07030

Stevens Institute of Technology
Attn: A. T. Chang
Castle Point Station
Hoboken, NJ 07030

Mechanical Technologies Inc.
Attn: M. S. Darlow
Latham, NY

Shaker Research Corporation
Attn: L. Lagace
Northway 10, Executive Park
Ballston Lake, NY 12019

Lockheed Palo Alto Research Labs
Attn: Dr. D. Bushnell
Palo Alto, CA 94304

Lockheed Missiles and Space Company
Huntsville Research & Eng. Center
Attn: H. B. Shirley
P. O. Box 1103
Huntsville, AL 18908

MacNeal-Schwendler Corporation
Attn: R. H. MacNeal
7442 North Figueroa Street
Los Angeles, CA 90041

MARC Analysis Research Corporation
Attn: T. B. Wertheimer
260 Sheridan Avenue, Suite 314
Palo Alto, CA 94306

United Technologies Research Center
Attn: Dr. A. Dennis, MS 18
East Hartford, CT 06108

DISTRIBUTION LIST (continued)

Ohio State University
Attn: A. W. Leissa
Columbus, OH 43210

University of California
Attn: L. A. Schmidt, Jr.
Mechanics & Structures Department
School of Eng. & Applied Science
Los Angeles, CA 90024

Columbia University
Attn: R. Vaicaitis
New York, NY 10027

Georgia Institute of Technology
School of Civil Engineering
Attn: S. N. Atluri
Atlanta, GA 30332

Georgia Institute of Technology
Attn: G. J. Simitses
225 North Avenue
Atlanta, GA 30332

Lawrence Livermore Laboratory
Attn: Library
P. O. Box 808, L-421
Livermore, CA 94550

Lehigh University Institute of
Fracture and Solid Mechanics
Attn: G. T. McAllister
Bethlehem, PA 18015

Materials Science Corporation
Attn: W. B. Rosen
1777 Walton Road
Blue Bell, PA 19422

National Bureau of Standards
Engineering Mechanics Section
Attn: R. Mitchell
Washington, D.C. 20234

Univ. of Dayton Research Institute
Attn: F. K. Bogner
Dayton, OH 45409

Worcester Polytechnic Institute
Dept. of Mechanical Engineering
Attn: Dr. J. H. Kane
100 Institute Road
Worcester, MA 01609

Purdue University
School of Aeronautics & Astronautics
Attn: C. T. Sun
West Lafayette, IN 47907

Texas A&M University
Aerospace Engineering Department
Attn: W. E. Haisler
College Station, TX 77843

Texas A&M University
Aerospace Engineering Department
Attn: J. M. Vance
College Station, TX 77843

V. P. I. and State University
Department of Engineering Mechanics
Attn: R. T. Haftka
Blacksburg, VA 24061

University of Arizona
College of Engineering
Attn: P. Wirsching
Tucson, AZ 87521

University of California
Department of Civil Engineering
Attn: E. Wilson
Berkeley, CA 94720

University of Kansas
School of Engineering
Attn: R. H. Dodds
Lawrence, KS 66045

DISTRIBUTION LIST (continued)

University of Virginia
School of Eng. & Applied Science
Attn: E. J. Gunter
Charlottesville, VA 22901

Northwestern University
Department of Civil Engineering
Attn: T. Belytschko
Evanston, IL 60201

Southwest Research Institute
P. O. Drawer 28510
6220 Culebra Road
San Antonio, TX 78284

Univ. of California at Santa Barbara
Dept. of Mech. & Environmental Eng.
Attn: Dr. G. N. Vanderplaats
Santa Barbara, CA